AD_____

GRANT NUMBER: DAMD17-94-J-4401

TITLE: The P53-Deficient Mouse as a Breast Cancer Model

PRINCIPAL INVESTIGATOR: Lawrence A. Donehower, Ph.D.

CONTRACTING ORGANIZATION: Baylor College of Medicine
Houston, TX 77030

REPORT DATE: October 1996

TYPE OF REPORT: Annual

PREPARED FOR: Commander
U.S. Army Medical Research and Materiel Command
Fort Detrick, Frederick, MD 21702-5012

REPORT DOCUMENTATION PAGE

Form Approved
OMB No. 0704-0188

1. AGENCY USE ONLY (Leave blank)	2. REPORT DATE	3. REPORT TYPE AND DATES COVERED
	October 1996	Annual (15 Sep 95 - 14 Sep 96)

4. TITLE AND SUBTITLE
The P53-Deficient Mouse as a Breast Cancer Model

5. FUNDING NUMBERS
DAMD17-94-J-4401

6. AUTHOR(S)
Lawrence A. Donehower, Ph.D.

7. PERFORMING ORGANIZATION NAME(S) AND ADDRESS(ES)
Baylor College of Medicine
Houston, TX 77030

8. PERFORMING ORGANIZATION REPORT NUMBER

9. SPONSORING/MONITORING AGENCY NAME(S) AND ADDRESS(ES)
Commander
U.S. Army Medical Research and Materiel Command
Fort Detrick, Frederick, MD 21702-5012

10. SPONSORING/MONITORING AGENCY REPORT NUMBER

11. SUPPLEMENTARY NOTES

12a. DISTRIBUTION/AVAILABILITY STATEMENT
Approved for public release;
distribution unlimited

12b. DISTRIBUTION CODE

13. ABSTRACT *(Maximum 200 words)*

The p53 tumor suppressor gene is mutated in almost half of all human cancers and in roughly 30-40% of breast cancers. In order to better understand the role of p53 mutation and loss in breast cancer progression, we have developed a mouse model which is genetically programmed to develop mammary cancer in the presence and absence of p53. By comparison of the mammary tumorigenesis process between the p53 positive and p53 negative animals we hope to obtain further insights into the mechanisms by which loss of p53 accelerates tumor progression. In the first two years of this grant we have shown that in the absence of p53 mammary tumors arise sooner and grow faster than mammary tumors with intact p53. We have also shown that tumors without p53 have higher levels of chromosomal instability and higher rates of cell proliferation than tumors with p53. Rates of apoptosis (programmed cell death) were shown to be low and not significantly different between p53 positive and negative tumors. Thus, our results appear to validate the model as useful in elucidating the role of p53 loss in the tumorigenesis process and underscore the likelihood that p53 has multiple functions in its prevention of tumor formation and progression.

14. SUBJECT TERMS	15. NUMBER OF PAGES
Breast Cancer	40
	16. PRICE CODE

17. SECURITY CLASSIFICATION OF REPORT	18. SECURITY CLASSIFICATION OF THIS PAGE	19. SECURITY CLASSIFICATION OF ABSTRACT	20. LIMITATION OF ABSTRACT
Unclassified	Unclassified	Unclassified	Unlimited

GENERAL INSTRUCTIONS FOR COMPLETING SF 298

The Report Documentation Page (RDP) is used in announcing and cataloging reports. It is important that this information be consistent with the rest of the report, particularly the cover and title page. Instructions for filling in each block of the form follow. It is important to ***stay within the lines*** to meet ***optical scanning requirements***.

Block 1. Agency Use Only *(Leave blank)*.

Block 2. Report Date. Full publication date including day, month, and year, if available (e.g. 1 Jan 88). Must cite at least the year.

Block 3. Type of Report and Dates Covered. State whether report is interim, final, etc. If applicable, enter inclusive report dates (e.g. 10 Jun 87 - 30 Jun 88).

Block 4. Title and Subtitle. A title is taken from the part of the report that provides the most meaningful and complete information. When a report is prepared in more than one volume, repeat the primary title, add volume number, and include subtitle for the specific volume. On classified documents enter the title classification in parentheses.

Block 5. Funding Numbers. To include contract and grant numbers; may include program element number(s), project number(s), task number(s), and work unit number(s). Use the following labels:

C	- Contract	PR	- Project
G	- Grant	TA	- Task
PE	- Program Element	WU	- Work Unit Accession No.

Block 6. Author(s). Name(s) of person(s) responsible for writing the report, performing the research, or credited with the content of the report. If editor or compiler, this should follow the name(s).

Block 7. Performing Organization Name(s) and Address(es). Self-explanatory.

Block 8. Performing Organization Report Number. Enter the unique alphanumeric report number(s) assigned by the organization performing the report.

Block 9. Sponsoring/Monitoring Agency Name(s) and Address(es). Self-explanatory.

Block 10. Sponsoring/Monitoring Agency Report Number. *(If known)*

Block 11. Supplementary Notes. Enter information not included elsewhere such as: Prepared in cooperation with...; Trans. of...; To be published in.... When a report is revised, include a statement whether the new report supersedes or supplements the older report.

Block 12a. Distribution/Availability Statement. Denotes public availability or limitations. Cite any availability to the public. Enter additional limitations or special markings in all capitals (e.g. NOFORN, REL, ITAR).

- DOD - See DoDD 5230.24, "Distribution Statements on Technical Documents."
- DOE - See authorities.
- NASA - See Handbook NHB 2200.2.
- NTIS - Leave blank.

Block 12b. Distribution Code.

- DOD - Leave blank.
- DOE - Enter DOE distribution categories from the Standard Distribution for Unclassified Scientific and Technical Reports.
- NASA - Leave blank.
- NTIS - Leave blank.

Block 13. Abstract. Include a brief *(Maximum 200 words)* factual summary of the most significant information contained in the report.

Block 14. Subject Terms. Keywords or phrases identifying major subjects in the report.

Block 15. Number of Pages. Enter the total number of pages.

Block 16. Price Code. Enter appropriate price code *(NTIS only)*.

Blocks 17. - 19. Security Classifications. Self-explanatory. Enter U.S. Security Classification in accordance with U.S. Security Regulations (i.e., UNCLASSIFIED). If form contains classified information, stamp classification on the top and bottom of the page.

Block 20. Limitation of Abstract. This block must be completed to assign a limitation to the abstract. Enter either UL (unlimited) or SAR (same as report). An entry in this block is necessary if the abstract is to be limited. If blank, the abstract is assumed to be unlimited.

FOREWORD

Opinions, interpretations, conclusions and recommendations are those of the author and are not necessarily endorsed by the US Army.

____ Where copyrighted material is quoted, permission has been obtained to use such material.

____ Where material from documents designated for limited distribution is quoted, permission has been obtained to use the material.

L.A.D. Citations of commercial organizations and trade names in this report do not constitute an official Department of Army endorsement or approval of the products or services of these organizations.

L.A.D. In conducting research using animals, the investigator(s) adhered to the "Guide for the Care and Use of Laboratory Animals," prepared by the Committee on Care and Use of Laboratory Animals of the Institute of Laboratory Resources, National Research Council (NIH Publication No. 86-23, Revised 1985).

____ For the protection of human subjects, the investigator(s) adhered to policies of applicable Federal Law 45 CFR 46.

L.A.D. In conducting research utilizing recombinant DNA technology, the investigator(s) adhered to current guidelines promulgated by the National Institutes of Health.

L.A.D. In the conduct of research utilizing recombinant DNA, the investigator(s) adhered to the NIH Guidelines for Research Involving Recombinant DNA Molecules.

LAD In the conduct of research involving hazardous organisms, the investigator(s) adhered to the CDC-NIH Guide for Biosafety in Microbiological and Biomedical Laboratories.

Lawrence A. Donehower 9/23/96

PI - Signature Date

TABLE OF CONTENTS

Progress Report: The p53-Deficient Mouse as a Breast Cancer Model

Principal Investigator: Lawrence A. Donehower, Ph.D.

Introduction:

The p53 tumor suppressor gene is mutated in roughly half of all human tumors examined to date (1). Approximately 30-40% of human breast cancers have p53 mutations, indicating loss of p53 function is a central event in breast cancer progression (1). Even in those breast cancers where p53 is wild type in structure, it may be abnormally stabilized or localized within the cell, suggesting possible disruption of p53-associated growth control pathways (2). In addition to its loss in spontaneously arising breast cancers, inherited mutations ofthe germ line p53 gene can also occur, giving rise to a familial cancer predisposition called Li-Fraumeni syndrome (3,4). The most frequently observed tumor in affected females of Li-Fraumeni families is breast cancer (5).

The role of p53 in the normal cell appears in large part to be that of a cell cycle checkpoint protein. In response to a variety of DNA damaging agents, p53 levels in the cell increase and mediate one of two cell fates: (i) arrest in G1 of the cell cycle, or (ii) apoptosis (6-8). The decision to undergo arrest versus apoptosis may rely on many factors, including cell type, growth factor levels, and abrogation of function in other growth-related genes, etc. Regardless of which decision is taken, the end result is to prevent the cell from DNA synthesis and division in the presence of damaged DNA templates (9). Thus, the cell is more likely to be spared oncogenic mutations which could lead to cancer. In the absence of p53 (which may occur in preneoplastic cells and does occur in p53-deficient mice), it is hypothesized that cells would be more likely to become tumorigenic through increased mutation rates and genomic instability (9).

The biochemical mechanisms through which p53 mediates its checkpoint functions are likely to be complicated, though clearly transcriptional regulation of key growth related genes is crucial for its G1 arrest function (8,10). Wild type p53 trans-activates the $p21^{WAF1/CIP1}$ gene, which encodes a potent inhibitor of G1 cyclin-dependent kinases (11,12). Transcriptional activation plays a role in p53-mediated apoptosis (13), though which p53 targets are critical for apoptosis are unclear. In other instances, it has been shown that p53 can mediate apoptosis in the absence of transcriptional activation, suggesting multiple mechanisms by which p53 effects apoptosis (14,15).

There is significant evidence that p53-mediated apoptosis may play an important role in suppression of tumors (16-18). Aberrant expression of certain oncogenes and tumor suppressor genes may induce high levels of p53 (19,20). When cells are induced to proliferate abnormally by these genes, p53 upregulation may induce apoptosis and thus protect the organism from early tumors. This role of p53 tumor suppression through apoptosis has been demonstrated in some mouse tumor models. In situations where Rb function is abrogated in a tissue, G1 arrest capability is often lost and these abnormally proliferating cells are induced to undergo apoptosis.

In the absence of p53, such Rb-deficient tissues may rapidly form aggressive tumors, arguing that attenuated apoptosis due to p53 loss is a rate limiting step in tumor formation (16-18).

Is apoptotic function the primary mechanism by which p53 regulates tumor progression or are there other mechanisms? A number of *in vitro* and *in vivo* studies suggest that loss or mutation of p53 may have additional important biological effects on tumor formation and progression (21). Some of these effects of p53 loss on tumor progression maby be: (1) increased rates of cell proliferation independent of apoptotic effects; (2) increased levels of genomic instability in the tumor cells which may lead to further oncogenic lesions; (3) increased rates of angiogenesis, allowing more nutrients to nascent tumor cells; and (4) increased invasiveness and metastases. All of these biological effects are measurable, and an important goal of this proposal is to assess all of these potential tumor progression mechanisms in the context of the *Wnt-1*/p53 tumor model described below.

Initially, to study the role of p53 in tumorigenesis, we developed a p53-deficient mouse by gene targeting methods (22). These mice contained either one (p53+/-) or two (p53-/-) inactivated p53 germ line alleles. In comparison to their normal littermates, the p53-deficient mice showed accelerated tumorigenesis. Half of all p53+/- mice developed tumors by 18 months of age, while 100% of p53-/- mice succumbed to tumors by 10 months of age (23,24). The spectrum of tumors was quite variable, though lymphomas and sarcomas were most frequently observed (23,24).

While the analysis of tumorigenesis in the p53-deficient mice has yielded a number of interesting insights, the study of spontaneous tumor formation in these animals has certain limitations if one wants to examine mechanistic questions in an efficient, well controlled manner. For example, the p53-deficient mice develop a wide array of tumors sometimes with a relatively long latency (particularly the p53+/- mice). Moreover, since p53+/+ mice rarely develop tumors, control tumors which develop in a p53-independent manner are difficult to obtain. To circumvent these disadvantages, investigators have taken two general approaches, either treating the p53-deficient mice with a tissue-specific carcinogen or crossing the p53-deficient mice to a tumor-susceptible transgenic mouse genetically programmed to develop a single tumor type. The resulting models usually develop a single tumor type in a relatively short amount of time and control p53+/+ tumors are available to compare to the p53-deficient tumors.

The model we chose for examination of the role of p53 loss in tumor progression was the *Wnt-1* transgenic/p53-deficient mouse (25). This model was generated by crossing our p53-deficient mice to mammary tumor susceptible *Wnt-1* transgenic mice (26). *Wnt-1* transgenic females, which contain a mouse mammary tumor virus long terminal repeat promoter driving the *Wnt-1* oncogene, specifically develop early mammary gland hyperplasia followed by mammary adenocarcinomas before 12 months of age in a stochastic manner (26). Thus, our prediction was that virtually all of the *Wnt-1* transgenic females would develop mammary adenocarcinomas either in the presence or absence of wild type p53. Such mice would be ideal for exploring the biological and genetic effects of p53 presence and absence in mammary tumor formation and progression.

Body:

Experimental Methods

Mice

The *Wnt-1* mice used in the crosses described here were the offspring of two *Wnt-1* males from line 303 described previously (Tsukamoto et al., 1988). These mice were of mixed SJL X C57/BL/6 genetic background. The p53-deficient mice were from a pure 129/Sv line of mice containing one or two germ-line *p53* null alleles (27). The two *Wnt-1* males were crossed to heterozygous (*p53*+/-) 129/Sv females to derive F1 mice of four possible genotypes (*p53*+/+; *Wnt-1 p53*+/+; *p53*+/-; *Wnt-1 p53*+/-). F1 *p53*+/- females were crossed to F1 *Wnt-1 p53* +/- males to obtain F2 mice that carried any of the *Wnt-1 p53* genotypes found in the F1 population as well as *Wnt-1 p53*-/- or *p53*-/- . To obtain larger numbers of mice with *p53*-/- genotypes with or without the *Wnt-1* transgene, F2 *p53*-/- females were mated to *Wnt-1 p53* -/- males. All of the mice were monitored visually twice weekly for the appearance of tumors for up to one year. When a tumor of roughly 0.5 centimeters in diameter was detected, the age of the mouse was recorded and used to generate the Kaplan-Meier plots in Fig. 1. Once a tumor reached 1.5-2 cm in diameter, the tumor-bearing mouse was sacrificed, and tissue sections removed for histopathology. The remainder of the tumor was frozen at -70°C for nucleic acid analyses.

Genotyping of Mice

We determined the *p53* and *Wnt-1* genotypes of the offspring from the crosses using previously described methods (25,26). Briefly, 1 cm of tail was clipped from weanling mice and incubated overnight at 55-60° C in 500 µl of tail lysis buffer (50 mM Tris-HCl pH 7.5, 50 mM EDTA pH 8.0, 100 mM NaCl, 5 mM DTT, 200 µg/ml Proteinase K). Lysates were extracted with phenol chloroform and precipitated in two volumes ethanol. Pellets were resuspended in 100 µl TE (10 mM Tris-HCl, pH 8.0, 1 mM EDTA). Five µl of each tail DNA was cleaved with Bam HI (2-16 hr at 37° C) and subjected to agarose gel electrophoresis on a 0.7% gel. The gel was then blotted to nylon membranes (Bio-Rad Zetaprobe membranes) and hybridized according to the Southern blot hybridization procedures of Reed and Mann (28). *Wnt-1* probes and p53 probes were utilized simultaneously in the hybridization and were labelled with ^{32}P with an oligo labelling kit provided by Boehringer-Mannheim. Filters were rinsed and subjected to autoradiography. The p53 wild type allele (5.0 kb), mutant p53 allele (6.5 kb), *Wnt-1* transgene (3.0 kb), and endogenous *Wnt-1* gene (2.0 kb) could easily be differentiated by this procedure.

Loss of Heterozygosity Assays

These assays were performed by Southern blot hybridization procedures identical to those described above for genotyping except that small pieces of

mammary tumor tissue were used instead of tail. Roughly half of the tumors displayed loss of the remaining wild type p53 allele while half retained it by Southern blot assay.

Tumor Transplantation Assays

Either 10^4, 10^5, or 10^6 tumor cells isolated from primary mammary tumors were transplanted into the inguinal mammary fat pads of female SCID hosts 8-16 weeks of age. These tumor cells developed into tumors whose diameter and growth rates were measured by calipers over a period of 6 weeks. The tumor cells were isolated from the tumors by mincing with a sterile razor blade followed by a 3 hour incubation at 37°C in DMEM:F12, collagenase and antibiotics as described by Kittrell et al. (29). The tumor cells were spun down and then rinsed three times with PBS containing 5% ABS to inactivate the Collagenase. The cells were then resuspended in DMEM:F12 and an aliquot was counted on a hemocytometer. Approximately 10 µl containing the appropriate number of cells were then injected into the inguinal fat pad of female SCID hosts.

Mitotic Index Counts

A determination of the number of mitotic figures in each tumor section was performed as follows: Mitotic figures (cells containing obvious condensed chromosomes in various stages of mitosis) were counted in 10 random high power fields at or near the edges of standard hematoxylin and eosin stained tumor cross sections.

BrdU Incorporation

BrdU incorporation was performed using the Cell Proliferation Kit from Amersham (RPN 20). Briefly, 1 ml of BrdU (from kit) per 50 grams body weight of the mouse was injected intraperitoneally. The labeling of cells was allowed to proceed for three hours at which time tumors were harvested and fixed in methacarn fixative solution overnight. Samples were then transferred to acetone for at least three hours and then stored in 95% ethanol until embedding in paraffin. Sections were stained for BrdU incorporation as follows: Samples were deparaffinized by washing twice in xylene, twice in 100% ethanol and once in 70% ethanol. Samples were then rehydrated in PBS for 20 minutes. Endogenous peroxidase activity was quenched by immersing samples in 3% hydrogen peroxide for five minutes followed by two 10 minute rinses in PBS. The samples were then incubated at 37° C for one hour with nuclease and Anti-BrdU antibody (Kit), followed by a 20 minute wash with PBST and 10 minutes with PBS. This was followed by incubation with the secondary antibody for 30 minutes at 37° C. Samples were then washed for 10 minutes with PBST and twice for 10 minutes with PBS. Substrate was provided in the form of DAB in 1x PBS for 10 minutes. Counterstaining is done with Methyl Green for 5 minutes followed by dipping in butanol, 100% ethanol, and xylene. Samples were then mounted with Permount.

Flow Cytometry

The DNA content of tumor samples was assessed in nuclei isolated from paraffin embedded samples based on a modification of Hedley's method (30). Nuclear suspensions were prepared from five 50 μm sections, a 4 μm section was cut before and after the 50 μm sections to confirm that histologically comparable sections were being used. The samples were deparaffinized using two 50 minute xylene washes at 25° C. The cells were then rehydrated using successive incubations with ethanol, two per dilution, 100%, 95%, 70%, 50% and distilled water. Between each concentration of ethanol there is a 50 minute incubation at 25° C to make a cell suspension. To make this a single cell suspension the cells were treated with a 0.5% pepsin solution at 37° C for 30 minutes. Filtration through a 74 μm mesh (Small Parts Inc., Miami, FL) resulted in a nuclear suspension which was stained using the Vindelov technique (31). For a procedural control fresh chicken erythrocyte nuclei (CEN) (Accurate Chemical & Scientific Co., Westbury, NY) were used. A five microliter solution of a 20,000,000 CEN/ml suspension was added to the sample prior to the DNA staining step.

The sample used for actual DNA flow analysis was acquired of a FACScan flow cytometer using the ModFitLT software with doublet discrimination from Becton Dickinson, San Jose, CA. Twenty thousand events were collected using the gating parameters of FL2-W versus FL2-A. Histograms were generated to determine the percentage of cells in each stage of the cell cycle. The Coefficient of Variation (CV) was determined for the diploid G0/G1 peak for all cases. Only those samples with CV's of less than 8% were used.

DNA Laddering Apoptosis Assay

Genomic DNA was isolated from frozen tumor tissue by methods similar to those described for the loss of heterozygosity procedure except that pelleting of the DNA utilized 30 minute centrifugations rather than five minute centrifugations. Twenty micrograms of total DNA from each tumor was then run out on a 1.5% agarose gel. The gel was blotted using standard Southern blot procedures (28) and probed using a total mouse genomic probe cleaved with Hae III and labelled with ^{32}P through the oligo labelling procedure with the High Prime labelling kit (Boehringer-Mannheim). Following autoradiography of the Southern blot, the radioactivity on the filters was imaged and quantitated using a Molecular Dynamics phosphorimager. The amount of hybridization in the low molecular weight ladder bands (apoptotic fragments) of each lane was divided by the total amount of hybridizing radioactivity (after subtracting background) in that lane to obtain an estimate of the percentage apoptotic DNA.

TUNEL Assay

The TUNEL assay was performed using the TACS™ 2 TdT *In Situ* Apoptosis Detection Kit (Trevigen, Gaithersburg, MD). Briefly, 4 μm sections on slides were deparaffinized by heating at 57° C for 20 minutes followed by placing in xylene for 10 minutes at room temperature. This was followed by another 5 minute xylene wash, a 5 minute 100% ethanol wash, a 5 minute 95% ethanol wash and a 70% ethanol wash

for a further 5 minutes. The slides were then rinsed twice in distilled water for 2 minutes each followed by a rehydration in PBS for 10 min. The samples were then digested for 10 minutes at room temperature with Proteinase K (Kit). Endogenous peroxidases were then quenched using 3% hydrogen peroxide for 5 minutes. The fragmented DNA ends present in apoptotic cells were then extended using TdT, Mn^{++}, biotin dNTP's in labeling buffer (Kit). This reaction mix was added to the samples and allowed to incubate at 37° C for 1 hour. The reaction was stopped and rinsed for 2 minutes in PBS. Streptavidin-HRP conjugate was then allowed to bind to the incorporated biotin-dNTPs at room temperature for 15 minutes. Substrate was provided in the form of DAB and the color reaction was allowed to proceed for 5 minutes at room temperature. Counterstaining was performed for 5 minutes with 1.0% methyl green (Kit). Samples were dipped briefly in butanol, 100% ethanol and xylene. Finally, samples were mounted with Permount.

Immunoblot detection of antibodies in mammary tumors

Equivalent amounts of protein from mouse tumors were separated by SDS polyacrylamide gel electrophoresis using 15% resolving gels, transferred to Immobilon P membrane (Millipore), and immunoblotted with either anti-mouse IgG (H+L) antibodies (Pierce), mouse kappa or lambda chain-specific antibodies (Cappell), or tumor bearing serum as previously described (32).

Telomerase, telomerase RNA, and telomere assays

The procedures for these assays are described in Broccoli et al. (33) and this reprint accompanies the progress report.

Results

(1) Data from first year of grant

To provide the background for the second year's progress, I felt it was necessary to briefly outline the progress in the first year. First, After crossing the p53-deficient mice to the *Wnt-1* transgenic mice, we monitored tumor formation in the various categories of offspring. We will focus on the *Wnt-1* transgenic females in the remainder of this report. Appearance of mammary tumors in the *Wnt-1* transgenic females was greatly accelerated in the absence of p53 (p53-/-) (Figure 1). All of the *Wnt-1* p53-/- females developed mammary adenocarcinomas by 15 weeks of age and very few developed lymphomas or other spontaneous tumors characteristic of the p53-/- mice. *Wnt-1* p53+/+ females showed a delayed mammary tumor incidence with 100% developing adenocarcinomas by 41 weeks of age. Interestingly, *Wnt-1* p53+/- females exhibited the same mammary tumor incidence as *Wnt-1* p53+/+ females, even in those cases where the p53+/- tumor showed loss of the remaining wild type allele.

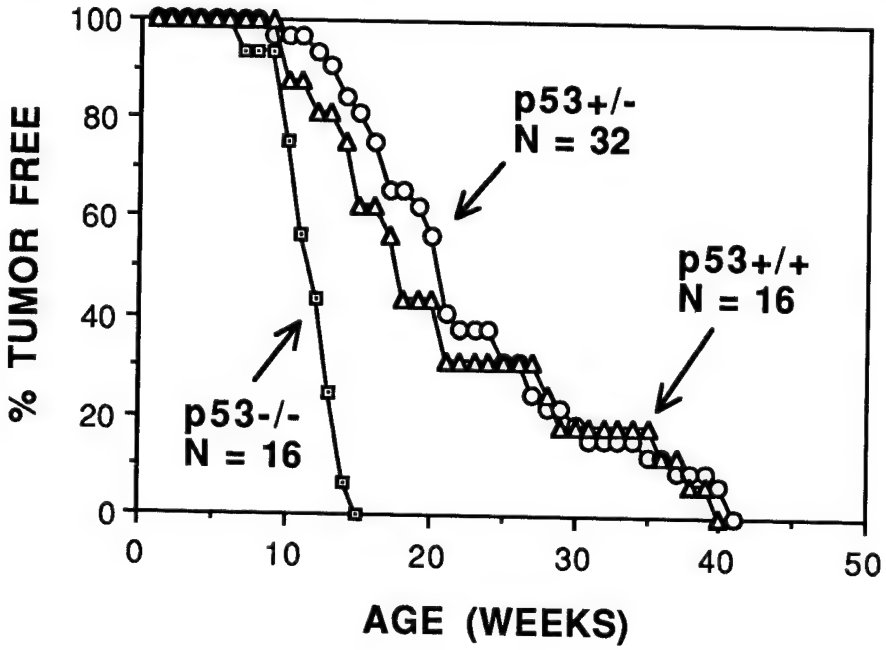

Figure 1.

In order to obtain insights into the mechanisms by which loss of p53 accelerated tumorigenesis, we analyzed the chromosomal complement of the *Wnt-1*-initiated mammary tumors in the presence and absence of p53. Previous *in vitro* studies had shown that the loss of p53 correlated with genomic instability. Using two different methods, classical cytogenetics and comparative genomic hybridization, we showed that loss or absence of p53 correlated quite well with increased genomic instability. A summary of the comparative genomic hybridization (CGH) results is shown on the next page (Table 1). It should be noted here that roughly half of the p53+/- tumors lose their remaining wild type allele (referred to as p53+/- LOH) and roughly half of the tumors appear to retain their wild type allele (referred to as p53+/- no LOH) as assayed by Southern blot hybridizaton. Sequencing of the p53 cDNA in four p53+/- tumors which retained the wild type allele showed no point mutations in the

remaining p53 gene and no downregulation of RNA expression, suggesting that wild type p53 function is retained in this category of p53+/- tumors.

Table 1. Summary of CGH Abnormalities in *Wnt-1* Mammary Adenocarcinomas

p53 Genotype	Tumors with Chromosome Abnormalities	Average Number of Chromosome Abnormalities per Tumor
p53+/+	2/6	0.3
p53+/- (no LOH)	2/4	1.0
p53+/- (LOH)	8/8	4.2
p53-/-	7/7	1.7

Tumors missing p53 (p53+/- LOH and p53-/-) showed significantly higher rates of chromosomal abnormalities, supporting the argument that loss of p53 promotes genomic instability. Surprisingly, Table 1 also shows that p53+/- tumors which lose their remaining wild type p53 allele have even more chromosomal abnormalities than p53-/- tumors. We are unsure why this would be so, but have speculated that p53+/- tumors have to undergo more mutations than p53-/- tumors because of environmental effects (i.e. organisms with no p53 may not be able to express certain extracellular inhibitors of tumor growth). Interestingly, the chromosomal abnormalities observed in the p53-deficient tumors were non-random in nature, suggesting a selection for certain chromosomal lesions which might provide a growth advantage. These results indicate that genomic instability does play a role in the progression of these tumors and that loss or absence of p53 may contribute to tumor progression in part through this mechanism.

(2) Results in second year of grant

In the second year of the grant our primary focus has been to determine some of the biological mechanisms by which loss or absence of p53 accelerates mammary tumorigenesis in the *Wnt-1* transgenic p53-deficient model. In the first year we concentrated on the involvement of genomic instability in tumor progression. In the second year we looked at three potential additional mechanisms: (i) cell cycle progression and proliferation; (ii) apoptosis (programmed cell death); and (iii) telomere and telomerase effects. The first two parameters are obviously of critical importance in the growth of the tumor as the tumor growth is a direct function of the rate of cell division minus the rate of cell death. There has been significant evidence from other

tumor models that loss of p53 is accompanied by attenuated apoptosis and that this event might be a rate limiting step in tumor formation (16-18).

(a) mammary tumor growth in the presence and absence of p53

Our first set of studies entailed some followup experiments on the tumor incidence data shown in Figure 1. The data in Figure 1 measures the time to first appearance of a visible tumor. Such curves may reflect early events in tumor formation. However, we wanted to more effectively measure the rates of tumor growth once the tumor is first observed. To do this, we measured the rate of tumor volume growth over time after initial observation. Tumor diameters in two dimensions were measured with calipers at weekly intervals and tumor volumes could then be estimated from these measurements. We found that while the rate of tumor volume growth for each p53 genotype was quite variable, the average growth of tumors missing p53 was faster than those containing p53 (Figure 2).

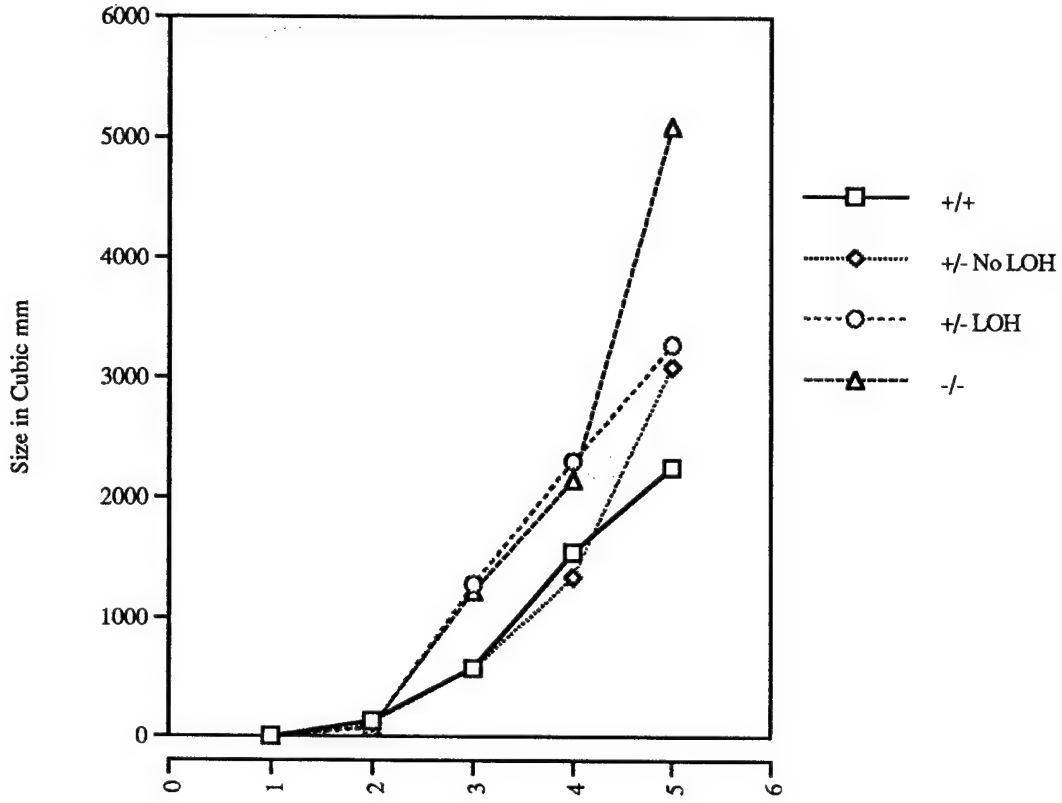

Figure 2.

We also performed tumor transplantation experiments in which we transplanted10^4, 10^5, or10^6 tumor cells from each tumor and injected them into the same inguinal mammary fat pad of genetically indentical recipient SCID mice. We

found that injection of 10^4 tumor cells often failed to produce any tumors after transplanting and 10^6 tumor cells formed tumors so rapidly that it was difficult to adequately differentiate tumor growth rates. However, virtually all of the transplantations with 10^5 tumor cells formed tumors which grew gradually enough to easily differentiate between fast growing and slow growing tumors. The transplant experiments also had a number of advantages over the primary tumor measurements. We were starting with the same number of tumor cells (10^5), injected into the same inguinal mammary fat pad, in genetically identical p53+/+ female SCID hosts between 8 and 16 weeks of age. Therefore, tumor growth rates are more likely to be dependent only on the properties of the tumor cells and not those of the host. The transplanted tumor cells were then monitored weekly for tumor outgrowth. Shown below are representative graphs for experiments in which 10^5 cells were transplanted (Figure 3).

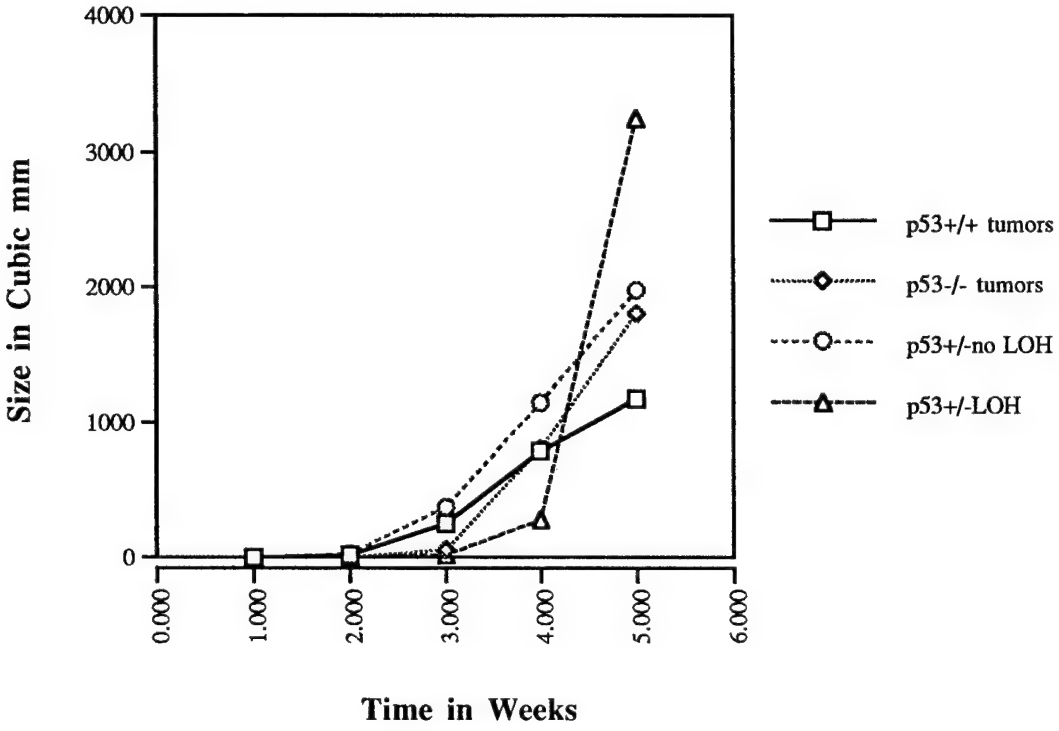

Figure 3.

The results shown in Figure 3 do not show the expected straightforward correlation between growth rate and p53 status. However, the p53+/+ tumors do show the slowest growth rates, and the p53+/- LOH tumors, after a slow start, have the fastest growth rate. Interestingly, the p53-/- tumor cells, which showed the fastest growth rate as primary tumors, showed slower growth rates than even the p53+/- no LOH tumors. We speculate that such slow rates may be attributable to an environmental effect. That is, organisms with intact p53 (such as the p53+/+ SCID hosts in these experiments) may release an inhibitor of tumor growth which p53-/- tumor cells have never been exposed to in the primary tumor. Therefore, it may take more time for the p53-/- tumor cells to evolve the appropriate mutations to overcome this inhibition. We plan more experiments in the future to corroborate this model. However, these experiments partially corroborate the primary tumor data that the absence of p53 tends to result in an increase in mammary tumor cell growth rates. In

the next sections we attempt to determine some of the mechanisms by which p53 loss may accelerate tumor cell growth rates.

(b) tumor cell proliferation and cell cycle progression

Probably the most obvious mechanism by which p53 loss could result in elevated tumor cell growth is through increased rates of cell division. We have shown previously that early passage p53-/- embryo fibroblasts divide more rapidly than their p53+/+ counterparts and have higher percentages of cells in S phase (34). To assess rates of cell division in the mammary tumors in the presence and absence of p53, we employed three different techniques: (i) mitotic index determinations; (ii) BrdU incorporation assays; and (iii) flow cytometry on fixed tumor cells. The mitotic index for each tumor was easily determined by counting the percentage of cells in a tumor in multiple microscopic fields which are clearly in mitosis through the identification of condensed chromatids in the fixed H & E sections. Two individuals performed these counts in a blinded fashion and obtained similar results. These are shown in Table 2 below.

Table 2. Mitotic Index of *Wnt-1* Mammary Adenocarcinomas

p53 Genotype	Mean Mitoses[a]	# Tumors Examined
p53+/+	16.7	9
p53+/- (No LOH)	23.8	6
p53+/- (LOH)	40.0	7
p53-/-	37.0	10

[a]Mean number of mitoses per 10 high power fields

The results above clearly indicate that cells which either lack or lose p53 show higher frequencies of mitosis as measured by this assay. To confirm that tumors without p53 also have higher percentages of cells in S phase, we employed a BrdU incorporation assay. BrdU was injected into the tumor bearing animals three hours prior to sacrifice. Tumor cells in S phase during this three hour window are detected by incubation of the tumor sections with an anti-BrdU antibody. Typical results for this assay on tumor sections are shown on the next page in Figure 4.

BrdU Incorporation into Tumors

p53 +/+ Mammary Tumor 100x

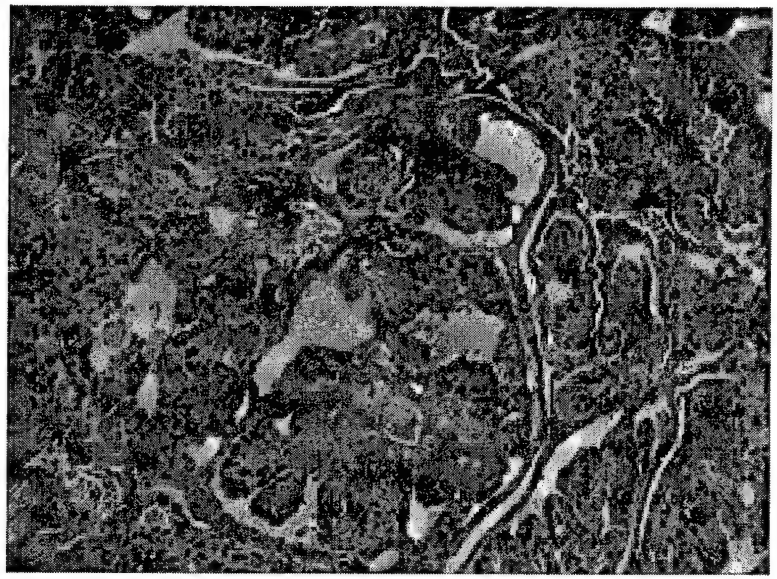

p53 -/- Mammary Tumor 100x

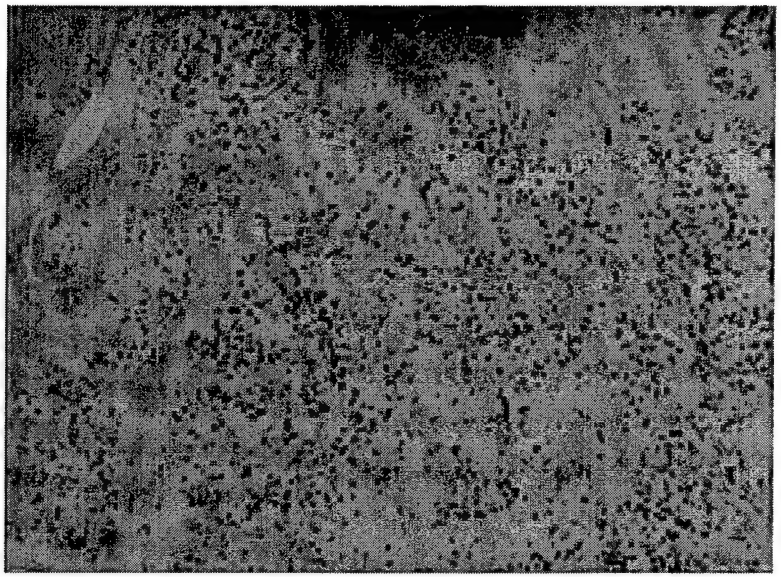

p53 +/+ Mammary Tumor 400x

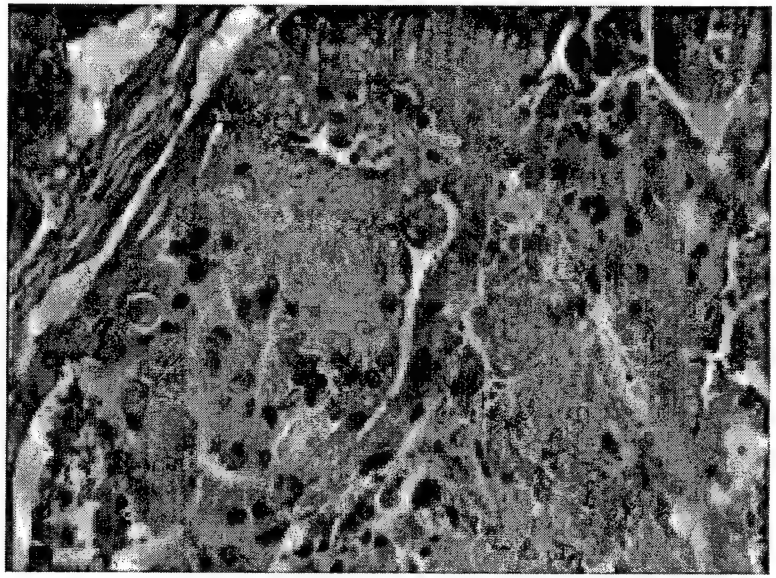

p53 -/- Mammary Tumor 400x

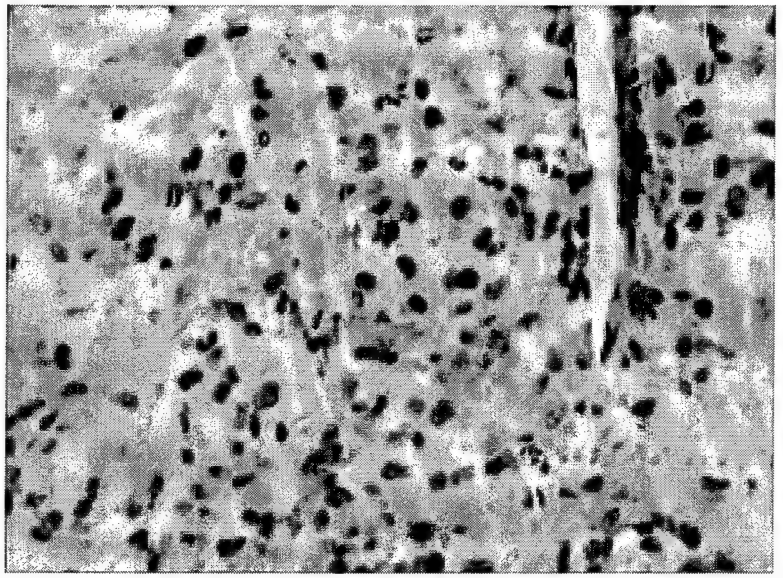

Figure 4.

Note that the p53-/- tumor appears to have more staining nuclei than the p53+/+ tumor. When results such as these were carefully quantitated, we again found that the p53+/- LOH and p53-/- tumors again had higher percentages of cells in S phase than p53+/+ and p53+/- no LOH tumors. While performing these assays, however, we found that our BrdU incorporation levels were lower than should have been expected. Subsequently, we have changed our fixative procedures and have successfully obtained higher levels of BrdU incorporation consistent with the observations of others. The BrdU incorporation results so far mirror those observed with the earlier fixative but sufficient numbers of tumors have not been analyzed yet to make any final conclusions.

Our final assay for cell proliferation involved flow cytometry on tumor cells from fixed sections of tumors to determine the DNA index and S-phase fraction. So far, sixteen *Wnt-1*/p53 tumors have been examined by flow cytometry and the results are indicated in Table 3 below. As expected, tumors losing or missing p53 have higher fractions of cells in S phase. p53+/- LOH show significantly higher S phase fractions than all other p53 genotypes. This result is consistent with the earlier mitotic index data. Interestingly, flow cytometry indicated that all four p53+/- LOH tumors were aneuploid while none of the other twelve tumors (including p53-/- tumors) appeared to have significant aneuploid fractions. This result is also consistent with the comparative genomic hybridization data presented in Table 1.

Table 3. Flow cytometry results on *Wnt-1* mammary adenocarcinomas

p53 genotype	Number	Mean S phase fraction	Aneuploidy
p53+/+	4	7.6%	0/4
p53+/- (no LOH)	3	8.7%	0/3
p53+/- (LOH)	4	18.7%	4/4
p53-/-	5	11.5%	0/5

(c) apoptosis

The growth rate of a tumor is likely to be influenced by at least two processes, the rate of cell division and the rate of cell death. We have shown strong evidence above that in the *Wnt-1* mammary tumor model the absence of p53 increases cell divison rates over those seen in tumors with intact p53. However, studies on other mouse tumor models have indicated that loss of p53 in a tumor cell may be accompanied by attenuated apoptosis and increased survival (16-18). To determine

whether p53 loss was accompanied by decreased apoptosis in our *Wnt-1*/p53 model we analyzed apoptosis by two methods, the TUNEL assay and DNA laddering assay. The TUNEL assay specifically labels nuclei with free DNA ends. Such free ends are signature events in apoptotic cells. We employed this assay on both normal and hyperplastic mammary glands and mammary tumors from the *Wnt-1*/p53 mice. Apoptosis levels were very low in both normal and hyperplastic mammary glands in the presence and absence of p53. Figure 5 on the next page shows representative pictures of hyperplastic mammary glands assayed by TUNEL. When mammary tumors were examined by TUNEL assay, we were surprised to find that *Wnt-1* tumors had low levels of apoptosis in both p53 positive and negative tumors and there was not a significant difference among the tumors.

The compilation of the TUNEL results for the tumor and non-tumor tissues are shown below in Table 3 and reveal that apoptosis levels remain relatively low and do not change significantly in the progression from normal mammary glands to malignant carcinoma.

Table 4. Summary of apoptosis results for TUNEL assay

Tissue Type	p53 Status	% Apoptotic Cells[a]	Sample #
Normal Mammary Gland	+/+	0.20	5
Hyperplastic Mammary Gland	+/+	0.57	9
Hyperplastic Mammary Gland	+/-	0.23	8
Hyperplastic Mammary Gland	-/-	0.33	3
Mammary Adenocarcinoma	+/+	0.75	7
Mammary Adenocarcinoma	+/- (no LOH)	0.44	6
Mammary Adenocarcinoma	+/- (LOH)	0.61	10
Mammary Adenocarcinoma	-/-	0.39	10

[a]Mean percentage of all samples in a category

p53 status plays little or no role in levels of apoptosis in the tumors in this model and this was further confirmed by a DNA laddering assay on the tumors. With this assay, there was not a great difference in the intensity of apoptotic DNA (represented by the discrete bands in the low molecular weight region of the gel following quantitation with the Molecular Dynamic Phosphorimager). If anything, we noted that p53-/- tumors had

Figure 5.

TUNEL Assay For Apoptosis

p53 +/+ Hyperplastic Mammary Gland 100x

p53 -/- Hyperplastic Mammary Gland 100x

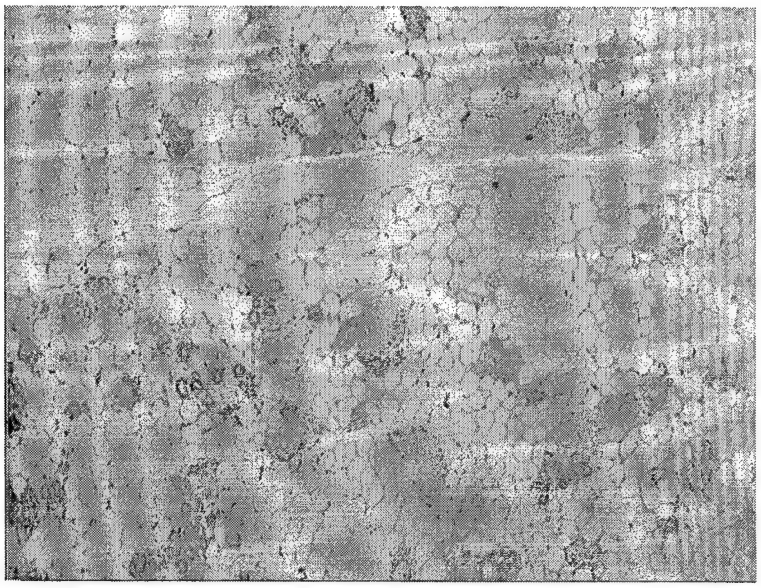

p53 +/+ Mammary Tumor 400x

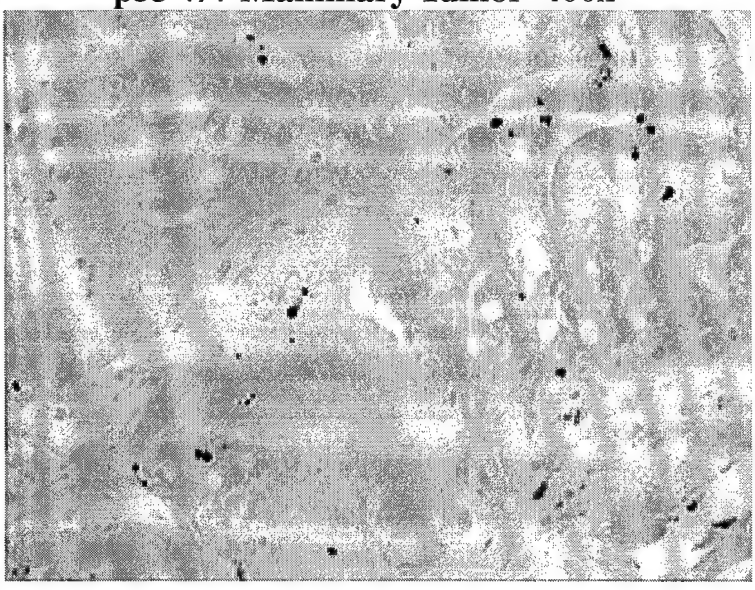

p53 -/- Mammary Tumor 400x

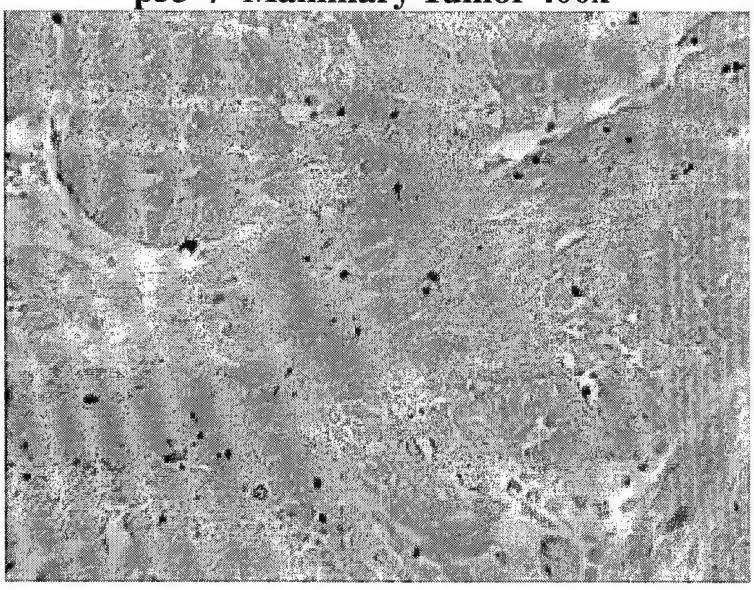

marginally higher percentages of apoptotic DNA compared to p53+/+ tumors (data not shown). Thus, our data supports the hypothesis that the increased tumor growth rate observed in the tumors lacking p53 is likely to a result of increased proliferation rate rather than decreased apoptotic function.

(d) antibody deposition in *Wnt-1* mammary adenocarcinomas

In a collaborative effort with Wafik El-Deiry at the University of Pennsylvania School of Medicine, we investigated $p21^{WAF1/CIP1}$ protein expression in p53-deficient tumors and *Wnt-1* mammary tumors. Using primarily immunoblot assays, assessment of p21 in the tumors tended to be variable and inconclusive. However, it was quickly noted that tumors from mice which had intact p53 (e.g. *Wnt-1* p53+/+ mice) had high levels of mouse light and heavy chain antibody deposition within the tumor tissue. In contrast, mice without p53 (e.g. *Wnt-1* p53-/- mice) had very low levels of antibody deposition within the tumor. Six of seven *Wnt-1* p53+/+ tumors had high levels of antibodies, while six of seven *Wnt-1* p53-/- tumors had very low levels of antibodies. Moreover, sera from tumor-bearing *Wnt-1* p53+/+ mice recognized multiple antigens in extracts from their own tumors. Sera from tumor-bearing *Wnt-1* p53-/- mice had substantially reduced reactivity with tumor antigens in their own tumors.

(e) telomere length, telomerase, and telomerase RNA

In collaboration with Titia de Lange at the Rockefeller, we were fortunate in being able to examine the contribution of telomerase and telomere degradation to tumor initiation and progression in the *Wnt-1* transgenic p53-deficient model (33). Some models of cancer formation implicate activation of telomerase activity as a critical event in tumor formation, since normal human cells in culture show both low telomerase activity and decreasing telomere size with passaging. Immortalized human cells and tumor cells often show increased telomere size and high levels of telomerase. It is postulated that early stage tumors may lose telomere function due to progressive shortening. This may lead to activation of DNA damage checkpoints, followed by cell cycle arrest and apoptosis. In tumors that have lost the ability to detect uncapped chromosome ends (e.g. p53-deficient cells), telomere malfunction may lead to genomic instability and accelerated tumor progression.

To test these possibilities, we compared telomere length, telomerase RNA, and telomerase activities in the normal mammary glands and mammary adenocarcinomas of the *Wnt-1* transgenic p53-deficient mice. Interestingly, mouse telomere length did not greatly vary in length between normal and tumor tissue, irrespective of p53 status, suggesting that decreasing telomere length is not an issue in mouse mammary tumorigenesis. Telomerase RNA was increased in amount in the mammary tumors compared to normal mammary glands, but p53 status had no apparent effect on the telomerase RNA levels. The most dramatic result was the high levels of telomerase activity observed in mammary tumors but not in the normal mammary glands or hyperplastic mammary glands (Table 5). There was a slight effect of p53 status on telomerase activity in the mammary tumors. p53-/- mammary tumors had roughly two fold more telomerase activity than p53+/+ tumors. However, it is unclear whether this

slight increase in telomerase activity may have a significant effect on tumor initiation and progression in the p53-/- mice. The most likely conclusion is that loss or absence of p53 has little or no effect on telomere status in mouse mammary tumors.

Table 5. Activation of telomerase in Wnt-1 mammary tumors in mice with different p53 genotypes

Type of sample	Telomerase activity[a]
p53-/- normal mammary gland	
MG 1-/-	9.3
MG 2-/-	4.5
MG 3-/-	18.3
Median	9.3
p53+/+ mammary tumor	
W2	17
W10	11
W30	36
W134	54
W151	24
Median	24
p53-/- mammary tumor	
W98	100
W121	94
W154	56
W177	14
W184	55
Median	54

[a] Telomerase activity is expressed as relative specific activity normalized to a mouse J558 standard. Average percent activity was determined from two to six assays.

CONCLUSIONS

The data presented in this report argue that p53 loss or absence may contribute to tumorigenesis by a variety of different mechanisms. Tumors without p53 appear to

grow and progress faster than tumors which contain p53. Surprisingly, while other mouse tumor models have demonstrated that loss of p53 is accompanied by attenuated apoptosis, we have shown in our model that apoptosis is likely to have little or no role in tumor progression. The reasons for the apoptotic independence in our model are unclear but it may have to do with the growth factor environment of the nascent tumor cells. *In vitro* assays often show that apoptosis can only be induced in the absence of certain growth factors. The nascent *Wnt-1*-initiated tumor cell is bathed in Wnt-1 growth factor and this may prevent any apoptotic pathways from being activated. However, this apoptotic independence makes our model particularly useful in teasing out other p53-dependent mechanisms which may influence tumor progression.

In the first two years of this grant we have attempted to identify some of these alternative mechanisms. Among these are increased genomic instability in the absence of p53 and increased proliferative capacity. Interestingly, while the tumors with the most genomic instability, the p53+/- (LOH) tumors, have the highest proliferative rates, they do not arise any sooner than p53+/+ tumors. This suggests that genomic instability plays a role in tumor progression but not tumor initiation. In addition, tumor cells missing or losing p53 appear to have a higher percentage of cells in S phase, suggesting that p53 may play a direct role in decreasing tumor growth rate through its growth arrest function (through checkpoint inhibition of progression through G1 and G2 or through direct inhibition of DNA replication).

We also examined the effects of p53 loss on telomere function in the presence and absence of p53 in our mammary tumor model. Telomeres themselves appear to maintain their structure during tumor progression, though telomerase activity is greatly increased. However, this telomerase increase appears to be mostly p53-independent, arguing against a role for p53 in this particular aspect of the tumorigenesis process.

Finally, through serendipity, we discovered that *Wnt-1* mice lacking p53 have greatly reduced amounts of heavy and light chain antibodies deposited in their tumors than *Wnt-1* mice with intact p53. The *Wnt-1* p53-/- mice also seem to be less able to mount an immune response to tumor antigens that *Wnt-1* p53+/+ mice are quite capable of recognizing. Such results argue that immune surveillance of nascent tumors in mice lacking p53 may be deficient and this may be part of the reason for the accelerated tumor incidence in *Wnt-1* p53-/- mice (see Figure 1).

In summary, in the second year of this grant, we have attempted to more fully answer mechanistic questions about the role of p53 loss in mammary tumor progression in our *Wnt-1* p53 model. We have shown that increased genomic instability and increased cell proliferation rates (independent of apoptosis) accompany loss of p53. Through collaborative efforts we have also examined telomere status and immune function in our model. In the next year, we hope to identify other mechanisms (e.g. increased angiogenesis) and examine particular genes which may mediate these important mechanisms. We do believe that the results achieved so far validate the *Wnt-1* transgenic p53-deficient mouse as a highly useful model for these types of studies.

References

1. Greenblatt MS, Bennett W, Hollstein M, Harris CC (1994) Mutations in the p53 tumor suppressor gene: clues to cancer etiology and molecular pathogenesis. Cancer Research 54:4855-4878

2. Moll U, Giou G, Levine A (1992) Two distinct mechanisms alter p53 in breast cancer: Mutation and nuclear exclusion. Proc Natl Acad Sci USA 89:7262-7266

3. Malkin D, Li FP, Strong LC, Fraumeni JF, Nelson CE, Kim DH, Kassell J, Gryka MA, Bischoff FZ, Tainsky MA, Friend SH (1990) Germ line p53 mutations in a familial syndrome of breast cancer, sarcomas, and other neoplasms. Science 250:1233-1238

4. Srivastava S, Zou Z, Pirollo K, Blattner W, Chang EH (1990) Germ-line transmission of a mutated p53 gene in a cancer-prone family with Li-Fraumeni syndrome. Nature 348:747-749

5. Malkin D (1994) Germline p53 mutations and heritable cancer. Annu. Rev. Genet. 28:443-465

6. Kastan MB, Canman CE, Leonard CJ (1995) p53, cell cycle control and apoptosis. Cancer and Metastasis Rev 14:3-15

7. Bates S, Vousden KH (1996) p53 in signaling checkpoint arrest or apoptosis. Curr Opin Genet & Develop 6:12-19

8. Ko LJ, Prives C (1996) p53: puzzle and paradigm. Genes & Develop 10:1054-1072

9. Lane DP (1992) p53, guardian of the genome. Nature 358:15-16

10. Gottlieb TM, Oren M (1996) p53 in growth control and neoplasia. BBA Rev Cancer 1287:77-102

11. Harper JW, Elledge SJ, Keyomarsi K *et al* (1995) Inhibition of cyclin-dependent kinases by p21CIP1/WAF1 *Molecular Biology of the Cell* **6** 387-400

12. El-Deiry WS, Tokino T, Velculescu VE *et al* (1993) WAF1, a potential mediator of p53 tumor suppression. *Cell* **76** 817-825

13. Sabbatini P, Lin J, Levine AJ, White E (1995) Essential role for p53-mediated transcription in E1A-induced apoptosis. Genes & Develop 9:2184-2192

14. Caelles C, Helmberg A, Karin M (1994) p53-dependent apoptosis in the absence of transcriptional activation of p53-target genes. Nature 370:220-223

15. Haupt Y, Rowan S, Shaulian E, Vousden KH, Oren M (1995) Induction of apoptosis in HeLa cells by trans-activation deficient p53. Genes & Development 9:2170-2183

16. Pan HC, Griep AE (1994) Altered cell cycle regulation in the lens of HPV-16 E6 or E7 transgenic mice - implications for tumor suppressor gene function in development Genes & Dev 8:1285-1299

17. Howes KA, Ransom N, Papermaster DS, Lasudry JGH, Albert, DM, Windle JJ (1994) Apoptosis or retinoblastoma - alternative fates of photoreceptors expressing the HPV-16 E7 gene in the presence or absence of p53 Genes & Dev 8:1300-1310

18. Symonds H, Krail L, Remington L, Saenz-Robles M, Lowe S, Jacks T, Van Dyke T (1994) p53-dependent apoptosis suppresses tumor growth and progression in vivo. Cell 78:703-711

19. Hermeking H and Eick D (1994) Mediation of c-myc-induced apoptosis by p53. Science 265:2091-2093

20. Lowe SW, Jacks T, Housman DE, Ruley HE (1994) Abrogation of oncogene-associated apoptosis allows transformation of p53-deficient cells. Proc Natl Acad Sci USA 91:2026-2030

21. Donehower LA (1996) Effects of p53 mutation on tumor progression: recent insights from mouse tumor models. BBA Rev Cancer 1242:171-176

22. Donehower LA, Harvey M, Slagle BL, McArthur MJ, Montgomery, CA Jr, Butel JS, Bradley A (1992) Mice deficient for p53 are developmentally normal but susceptible to spontaneous tumours. Nature 356:215-221

23. Harvey M, McArthur MJ, Montgomery CA, Butel JS, Bradley A, Donehower LA (1993) Spontaneous and carcinogen-induced tumorigenesis in p53-deficient mice. Nature Genet 5:225-229

24. Donehower LA, Harvey M, Vogel H, McArthur MJ, Montgomery CA Jr, Park SH, Thompson T, Ford RJ and Bradley A (1995) Effects of genetic background on tumorigenesis in p53-deficient mice. Mol Carcinog 14:16-22

25. Donehower LA, Godley LA, Aldaz CM, Pyle R, Shi Y-P, Pinkel D, Gray J, Bradley A, Medina D, Varmus HE (1995) Deficiency of p53 accelerates mammary tumorigenesis in *Wnt-1* transgenic mice and promotes chromosomal instability. Genes & Dev 9:882-895.

26. Tsukamoto AS, Grosschedl R, Guman RC, Parslow T, Varmus HE (1988) Expression of the *int-1* gene in transgenic mice is associated with mammary gland hyperplasia and adenocarcinomas in male and female mice. Cell 55:619-625

27. Harvey M, McArthur MJ, Montgomery CA, Bradley A, Donehower LA (1993) Genetic background alters the spectrum of tumors that develop in p53-deficient mice. FASEB J 7:938-943

28. Reed KC, Mann DA (1985) Rapid transfer of DNA from agarose gels to nylon membranes. Nucleic Acids Res 13:7207-7221

29. Kittrell FS, Oborn CJ, Medina D (1992) Development of mammary preneoplasias *in vivo* from mouse mammary epithelial cell lines *in vitro* . Cancer Research 52:1924-1932

30. Hedley DW, Friedlander ML, Taylor IW, Rugg CA, Musgrove EA (1993) Method of analysis of cellular DNA content of paraffin-embedded pathological material using flow cytometry. J Histochem Cytochem 21:1333-1335.

31. Vindelov LL, Christensen IJ, Nissen NI (1993) A detergent-trypsin method for the preparation of nuclei for flow cytometric DNA analysis. Cytometry 3:323-327

32. El-Deiry WS, Harper JW, O'Connor PM, Velculescu VE, Canman CE, Jackman J, Pietenpol JA, Burrell M, Hill DE, Wang Y, Wiman KG, Mercer WE, Kastan MB, Kohn KW, Elledge SJ, Kinzler KW, Vogelstein B (1994) WAF1/CIP1 is induced in p53-mediated arrest and apoptosis. Cancer Res 54:1169-1174

33. Broccoli D, Godley LA, Donehower LA, Varmus HE, de Lange T (1996) Telomerase activation in mouse mammary tumors: lack of detectable telomere shortening and evidence for regulation of telomerase RNA with cell proliferation. Mol Cell Biol 16:3765-3772

34. Harvey M, Sands AT, Weiss RS, Hegi M, Wiseman RW, Panayotis P, Biovanella BC, Tainsky MA, Bradley A, Donehower LA (1993) In vitro growth characteristics of embryo fibroblasts isolated from p53-deficient mice. Oncogene 8:2457-2467

Appendix:

Two reprints published in the last year which describe some of the work outlined above are appended here:

Donehower LA, Godley LA, Aldaz CM, Pyle R, Shi YP, Pinkel D, Gray J, Bradley A, Medina D, Varmus HE (1996) The role of p53 loss in genomic instability and tumor progression in a murine mammary cancer model. In Genetics and Cancer Susceptibility: Implications for Risk Assessment, Prog Clin Biol Res 395, pp.1-11.

Broccoli D, Godley LA, Donehower LA, Varmus HE, de Lange T (1996) Telomerase activation in mouse mammary tumors: lack of detectable telomere shortening and evidence for regulation of telomerase RNA with cell proliferation. Mol Cell Biol 16:3765-3772.

MOLECULAR AND CELLULAR BIOLOGY, July 1996, p. 3765–3772 Vol. 16, No. 7
0270-7306/96/$04.00+0

Telomerase Activation in Mouse Mammary Tumors: Lack of Detectable Telomere Shortening and Evidence for Regulation of Telomerase RNA with Cell Proliferation

D. BROCCOLI,[1] L. A. GODLEY,[2,3] L. A. DONEHOWER,[4] H. E. VARMUS,[2] AND T. DE LANGE[1]*

Laboratory for Cell Biology and Genetics, The Rockefeller University, New York, New York 10021[1]; Division of Basic Science, National Cancer Institute, Bethesda, Maryland 20892[2]; Department of Biochemistry and Biophysics, University of California at San Francisco, San Francisco, California 94143[3]; and Division of Molecular Virology, Baylor College of Medicine, Houston, Texas 77030[4]

Received 22 January 1996/Returned for modification 20 March 1996/Accepted 3 April 1996

Activation of telomerase in human cancers is thought to be necessary to overcome the progressive loss of telomeric DNA that accompanies proliferation of normal somatic cells. According to this model, telomerase provides a growth advantage to cells in which extensive terminal sequence loss threatens viability. To test these ideas, we have examined telomere dynamics and telomerase activation during mammary tumorigenesis in mice carrying a mouse mammary tumor virus long terminal repeat-driven *Wnt-1* transgene. We also analyzed *Wnt-1*-induced mammary tumors in mice lacking p53 function. Normal mammary glands, hyperplastic mammary glands, and mammary carcinomas all had the long telomeres (20 to 50 kb) typical of *Mus musculus* and did not show telomere shortening during tumor development. Nevertheless, telomerase activity and the RNA component of the enzyme were consistently upregulated in *Wnt-1*-induced mammary tumors compared with normal and hyperplastic tissues. The upregulation of telomerase activity and RNA also occurred during tumorigenesis in p53-deficient mice. The expression of telomerase RNA correlated strongly with histone H4 mRNA in all normal tissues and tumors, indicating that the RNA component of telomerase is regulated with cell proliferation. Telomerase activity in the tumors was elevated to a greater extent than telomerase RNA, implying that the enzymatic activity of telomerase is regulated at additional levels. Our data suggest that the mechanism of telomerase activation in mouse mammary tumors is not linked to global loss of telomere function but involves multiple regulatory events including upregulation of telomerase RNA in proliferating cells.

Telomerase is a cellular RNA-dependent DNA polymerase that can maintain the tandem arrays of telomeric repeats at eukaryotic chromosome ends (reference 26; reviewed in references 6 and 25). Human and mouse telomerases elongate the 3′ ends of chromosomes with strings of TTAGGG repeats (49, 50). This motif is dictated by a short template sequence within the RNA components of mammalian telomerases (7, 23). When telomerase is absent, chromosomes show progressive terminal sequence loss with cell divisions (23, 46, 57), probably reflecting the fact that the chromosomal replication machinery cannot duplicate DNA ends (61). The maintenance of the telomeric repeat array and its associated protein complex is essential for chromosome stability. Uncapped chromosomes are sensitive to degradation and fusion and can activate DNA damage checkpoints (40, 45, 54). Because of its ability to replenish lost telomeric sequences, telomerase is thought to be required for long-term cell proliferation.

Human telomerase has been implicated in cellular immortalization and tumorigenesis. High levels of telomerase activity have been demonstrated in immortalized cell lines (16, 17, 34, 49) and in the majority of human cancers (references 19 and 34; reviewed in reference 29). In normal human cells, telomerase activity is lower (9, 18, 31) or not detectable (19, 34). These variations in telomerase activity correlate with the dynamics of human telomeres. Telomere shortening at a rate of 50 to 200 bp per population doubling is a general phenomenon in normal human somatic cells (reference 28; reviewed in reference 29). In contrast, immortalized cell lines with high telomerase activity have stable telomeres or show telomere elongation (16, 17, 19, 39). One explanation for the increased telomerase activity in cancer is that restored telomeres confer a selective growth advantage during tumor progression (reviewed in reference 20). According to this model, telomere shortening in the early stages of tumor development results in loss of telomeric function, possibly because of a failure to engage the telomere-binding protein, hTRF (13). This in turn leads to the activation of DNA damage checkpoints, followed by cell cycle arrest and possibly apoptosis. In tumors that have lost the ability to detect uncapped chromosome ends, telomere malfunction might lead to extreme genome instability. Cells with high levels of telomerase activity may not experience the decreased viability associated with telomere malfunction and eventually dominate the later stages of tumorigenesis.

In order to test the idea that telomere attrition drives selection of telomerase-positive tumor cells, we have focused on telomere dynamics and telomerase activation in a mouse tumor model. Mouse telomerase activity has been demonstrated in a number of immortalized cells, tumors, and normal tissues (12, 50, 51). However, unlike human somatic cells in which the telomeres are composed of 5 to 10 kb of TTAGGG repeats (2, 3, 21), murine (*Mus musculus*) tissues have telomeres that are remarkably long, with telomeric tracts in the 20- to 50-kb range (37, 58). Since there is no indication for accelerated telomeric decline in the murine soma (37), it is expected that the telomeric tracts will not be depleted during tumor development, thereby obviating the need for increased telomere maintenance during tumorigenesis.

* Corresponding author. Mailing address: Box 159, Laboratory for Cell Biology and Genetics, The Rockefeller University, 1230 York Ave., New York, NY 10021. Phone: (212) 327-8146. Fax: (212) 327-7147. Electronic mail address: delange@rockvax.rockefeller.edu.

We have employed a murine system in which mammary tumors are induced by a mouse mammary tumor virus long terminal repeat-driven *Wnt-1* transgene, which results in ectopic expression of the *Wnt-1* proto-oncogene in mammary tissue and salivary glands (60). *Wnt-1* transgenic animals have hyperplastic mammary glands and are predisposed to the development of mammary adenocarcinomas. The stochastic appearance of these tumors is consistent with the idea that tumor formation requires alterations in addition to expression of *Wnt-1* in the mammary glands. Candidate cooperating genes (such as *int-2*, *fgf-3*, and *fgf-4*) have been identified elsewhere (41, 43, 55). *Wnt-1*-induced tumorigenesis is strongly accelerated in animals lacking a functional *p53* gene, possibly because of increased genomic instability (22). p53-deficient tumors display multiple karyotypic abnormalities, including aneuploidy, dicentric chromosomes, amplifications, and deletions (22).

Here we report that the telomerase activity in *Wnt-1* tumors was increased 10- to 20-fold relative to that measured in normal and hyperplastic mammary glands. Telomerase RNA levels were elevated twofold in the tumors and correlated with the expression of histone H4 mRNA in each of the tissues. The results indicate that telomerase activation in these tumors includes at least two regulatory events, one of which involves upregulation of the telomerase RNA with cellular proliferation. The average telomere array size was not appreciably altered during tumorigenesis. Since telomerase activation does not appear to be selected through global telomere shortening, upregulation of telomerase in tumors may serve a role other than maintenance of telomere length.

MATERIALS AND METHODS

Cell lines and mouse strains. The mouse myeloma cell line J558 (ATCC TIB6) was cultured in Dulbecco modified Eagle medium supplemented with 10% bovine calf serum, antibiotics, and glutamine. The transgenic mice used in this study have been previously described (22, 60). Normal mammary glands described in Table 1 were derived from SJL mice. *Wnt-1* transgenic mice used in this study have been backcrossed to the SJL strain for at least 10 generations; all hyperplastic mammary glands and mammary tumors described in Table 1 were harvested from these animals. For the p53-related studies, *Wnt-1* transgenic mice were crossed to p53-deficient mice of 129/Sv genetic background (22) and the resulting progeny were interbred. *Wnt-1* transgenic offspring of $p53^{+/+}$, $p53^{+/-}$, and $p53^{-/-}$ genotypes were monitored for mammary tumors. Tumors of 1.5 to 2.0 cm in diameter were harvested. A portion of the tumor was fixed and subjected to histopathological analysis to confirm the malignancies, and the remainder was frozen for the analysis performed here.

Protein extracts. All procedures were conducted at 4°C. Cell extract from the J558 cell line was prepared as previously described with 3-[(3-cholamidopropyl)-dimethylammonio-1-propanesulfonate] (CHAPS) detergent buffer (34). Extracts from frozen solid mammary tissues were prepared by disrupting 100 to 250 mg of tissue in 0.25 to 1 ml of CHAPS buffer with a mechanical homogenizer (9, 34). The suspension was mixed gently for 30 min and centrifuged at 100,000 × *g* in a Beckman TL 100.3 rotor for 30 min. For samples from which DNA plugs for pulsed-field gradient electrophoresis (see below) were prepared, the lysate was centrifuged at setting 4 in an Eppendorf microcentrifuge for 15 min to collect the nuclei before centrifugation of the supernatant at 100 K. For a subset of the preparations, one-half of the S100 was flash frozen while the remaining supernatant was first dialyzed against 50 mM KCl–20 mM HEPES(*N*-2-hydroxyethylpiperazine-*N'*-2-ethanesulfonic acid)-KOH (pH 7.9)–0.2 mM EDTA–0.2 mM EGTA [ethylene glycol-bis(β-aminoethyl ether)-*N,N,N',N'*-tetraacetic acid]–1 mM dithiothreitol–0.5 mM phenylmethylsulfonyl fluoride–20% glycerol for 2 h. In general, dialysis did not affect the telomerase activity but did remove nonspecific inhibitors of the reactions involved in the telomeric repeat amplification protocol (TRAP) present in some of the samples. Protein concentrations were determined by the Bradford assay (Bio-Rad) and bovine serum albumin as a standard. Western blot (immunoblot) analysis using an antibody which recognizes the heterogeneous nuclear ribonucleoprotein particle D group (32) was used to confirm protein concentrations and establish the absence of protein degradation.

Telomerase assay. Telomerase activity was detected by the PCR-based TRAP assay (34) with modifications and quantitation procedures as described previously (9). To measure telomerase activity, extract from each sample was first titrated between 0.1 and 1 μg to determine the protein range at which the TRAP products were proportional to the amount of protein. As was previously noted for human cell extracts (9, 63), the TRAP assay of mouse telomerase is quantitative when 0.05 to 1.0 μg of protein is assayed per reaction. TRAP assay products were visualized, and quantitation was done with a PhosphorImager and ImageQuant software (Molecular Dynamics). Telomerase activity was determined by summing the amount of signal present in TRAP assay products and correcting for background. The summed signal was then normalized to the amount of protein used to yield specific telomerase activities. The relative specific telomerase activity was determined by comparing the normalized TRAP product signals of experimental extracts with the normalized TRAP product signal obtained by using J558 extract from an assay performed in parallel. The level of specific telomerase activity in J558 was set to 100% in each assay, and the relative specific telomerase activities of the experimental extracts are expressed as a percentage of the specific telomerase activity found with the J558 standard. For each sample, the relative specific telomerase activity was determined from two to six independent assays. Similar amounts of protein were used in J558 and experimental extracts, precluding the need for extensive extrapolation. However, assays using different protein concentrations within the linear range of the dose-response curve of the assay resulted in similar values for the relative specific telomerase activity of any given sample. Samples with low levels of telomerase activity were mixed with the J558 standard to determine whether they contained an inhibitor of telomerase. None of the samples discussed in this study contained an inhibitor of the J558 telomerase standard.

Pulsed-field gel electrophoresis and genomic blotting. Nuclear pellets (see above) were washed three times in phosphate-buffered saline, cast in low-melting-point agarose plugs, and treated as previously described (1, 37). Restriction endonuclease digestions with *Mbo*I, *Rsa*I, and *Bam*HI were carried out according to manufacturers' recommendations. DNA was resolved on 1% agarose–0.5× Tris-borate-EDTA gels with a contour-clamped homogeneous electric field–DRII apparatus (Bio-Rad) for 20 h at 180 V with a constant pulse time of 5 s at 13°C. The DNA was subjected to acid depurination and transferred to Hybond N membranes (Amersham) by standard procedures. The telomeric oligonucleotide $(TTAGGG)_4$ was 5′ end labeled with [γ-^{32}P]ATP and T4 polynucleotide kinase. Hybridizations were carried out as described previously (38) at 65°C. The filters were washed in 4× SSC (1× SSC is 0.15 M NaCl plus 0.015 M sodium citrate)–0.1% sodium dodecyl sulfate (SDS) at 65°C prior to exposure to autoradiographic film.

RNA analysis. RNA was extracted from solid tissues by disrupting the tissue on ice with a mechanical homogenizer in 10 volumes of 6 M urea–3 M LiCl as described previously (5). RNAs (15 μg) were fractionated on 1% agarose-formaldehyde gels and transferred to Nytran membranes (Schleicher and Schuell) in 20× SSC. The mouse telomerase RNA probe (mTR [7]) and the histone H4 mRNA probe (kindly provided by N. Heintz, Rockefeller University) were labeled by the random priming reaction with 50 ng of isolated insert, [α-^{32}P]dCTP and [α-^{32}P]dGTP, and Klenow enzyme. Antisense oligonucleotides complementary to the mouse 7SK RNA polymerase III transcript (5′ CAGCCAGAT CAGCCGAATCAACCCTG 3′ and 5′ TGGACCTTGAGAGCTTGTTTGG AGG 3′ [48]) were 5′ end labeled with [γ-^{32}P]ATP and T4 polynucleotide kinase. Membranes were hybridized sequentially with the mTR and H4 probes as described previously (14) at 65°C with intervening removal of the probe by boiling in 2 mM sodium phosphate buffer (pH 7.2)–15 mM NaCl–0.5% SDS. Final washes were at 65°C in 40 mM sodium phosphate buffer (pH 7.2)–1 mM EDTA–1% SDS. Hybridization and washes with the 7SK probes were carried out as described above for the $(TTAGGG)_4$ oligonucleotide (above). Membranes were exposed to autoradiographic film for the generation of the data in Fig. 3 and to PhosphorImager screens (Molecular Dynamics) for quantitation.

RESULTS

Mouse telomeres do not shorten detectably during tumorigenesis. Telomeric restriction fragments were analyzed by pulsed-field gradient gel electrophoresis of DNA from normal and hyperplastic mammary glands and mammary tumors. In order to detect telomeric loci, the DNAs were digested with frequently cleaving restriction endonucleases (*Mbo*I or *Rsa*I) and probed with a telomere-specific oligonucleotide (Fig. 1). As expected, on the basis of previous reports of *M. musculus* telomeres (37, 58), the bulk of the telomeric fragments migrate in the 15- to 100-kb range with a peak of hybridization intensity around 25 to 30 kb. These DNA fragments have been shown to originate from the physical ends of chromosomes, on the basis of the telomere-specific in situ hybridization pattern of TTAGGG repeats (24, 47) and the sensitivity of these loci to exonuclease BAL 31 (37, 58). The largest telomeric fragments (50- to 150-kb range) in part originate from centromere-proximal telomeres and contain pericentromeric satellite sequences (36). These regions show a high degree of polymorphism between inbred strains as well as between individual mice (36, 37, 58) (Fig. 1).

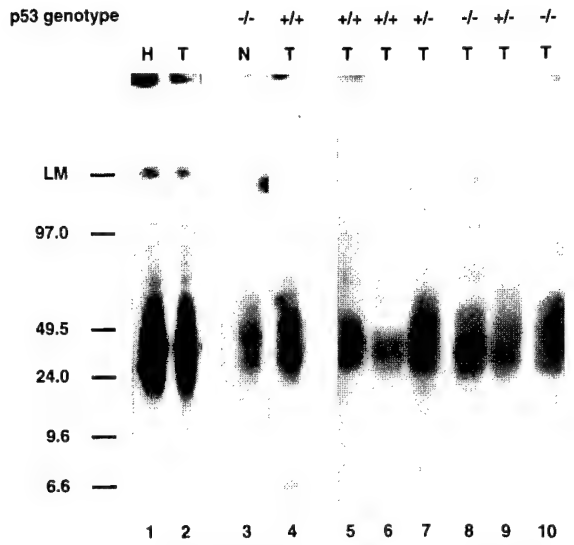

FIG. 1. Absence of telomere shortening during mouse mammary tumorigenesis. DNAs from normal mammary glands (N), hyperplastic mammary glands (H), and mammary tumors (T) were cleaved with either *Mbo*I (lanes 1 to 4) or *Rsa*I (lanes 5 to 10), resolved on contour-clamped homogeneous electric field gels, and annealed to a $(TTAGGG)_4$ probe. The DNAs in lanes 1 and 2 are derived from the same *Wnt-1* transgenic mouse. The *p53* genotype of the mice is indicated above the lanes for those samples that originated from crosses involving mice with p53 deficiencies. The lanes contained similar amounts of DNA with the exception of lane 6, which was slightly underloaded. The fragments in the 4- to 10-kb range are thought to be derived from chromosome-internal telomere-related sequences on the basis of their discrete size and their apparent identical size in different mice. The migration and molecular size (kilobases) of marker DNAs are indicated (LM is the limit of mobility).

Telomere size was found to be very similar in four normal mammary glands from control SJL mice, in four *Wnt-1*-induced hyperplastic mammary glands, and in four mammary tumors from *Wnt-1* transgenic mice. In each case, the bulk of telomeric fragments migrated in the 25- to 30-kb range (Fig. 1 and data not shown). This was true for DNA samples cleaved with *Mbo*I as well as for those cleaved with *Rsa*I and *Bam*HI. A side-by-side comparison of the telomeric restriction fragment patterns of a hyperplastic mammary gland and a mammary carcinoma derived from a single mouse is shown in Fig. 1. No alteration in telomere length was detectable in this or other tumor samples. In addition, we failed to detect changes in the length of the telomeric fragments or their annealing to TTAGGG repeat probes in three normal mammary glands and eight mammary carcinomas from mice with heterozygous or homozygous *p53* deletions (Fig. 1 and data not shown).

In human cells, increased chromosome instability occurs when the bulk of the telomeres have shortened to less than 2 kb of TTAGGG repeats (16). The data on the transgenic mice presented here are incompatible with such a dramatic decline and argue against transitory changes in telomere length during tumorigenesis in this system. Although we cannot rule out loss of a few kilobases from one or more telomeres, this level of shortening is unlikely to have compromised telomere function since at least 20 kb of TTAGGG repeats remains at the chromosome ends.

Elevated telomerase activity in mammary tumors. Telomerase activity was detectable by the PCR-based TRAP assay (34) in each of 15 normal mammary glands, 8 hyperplastic mammary glands, and 24 mammary tumors (Fig. 2). In each case, the activity resulted in the 6-nucleotide (nt) ladder typical of telomerase, and in each case pretreatment of the extract with RNase A inhibited the formation of TRAP products (Fig. 2 and data not shown).

Quantitative analysis was carried out to determine the relative enzyme activity in the extracts. We have previously shown that differences in telomerase activity between human tissue extracts can be determined in a quantitative manner with the TRAP assay and an internal standard (9). Similarly, we found that the telomerase levels in mouse cell extracts can be quantitated in relation to a standard (see Materials and Methods section for details). By this method, the specific telomerase activity (TRAP assay products per microgram of protein) in each extract is compared with a standard extract derived from the murine J558 cell line (Fig. 2). The relative specific activity (averaged from two to five independent assays) is expressed as a percentage of the specific telomerase activity found in the J558 standard (Table 1). For each sample, an RNase A digestion is included to confirm that the TRAP products are attrib-

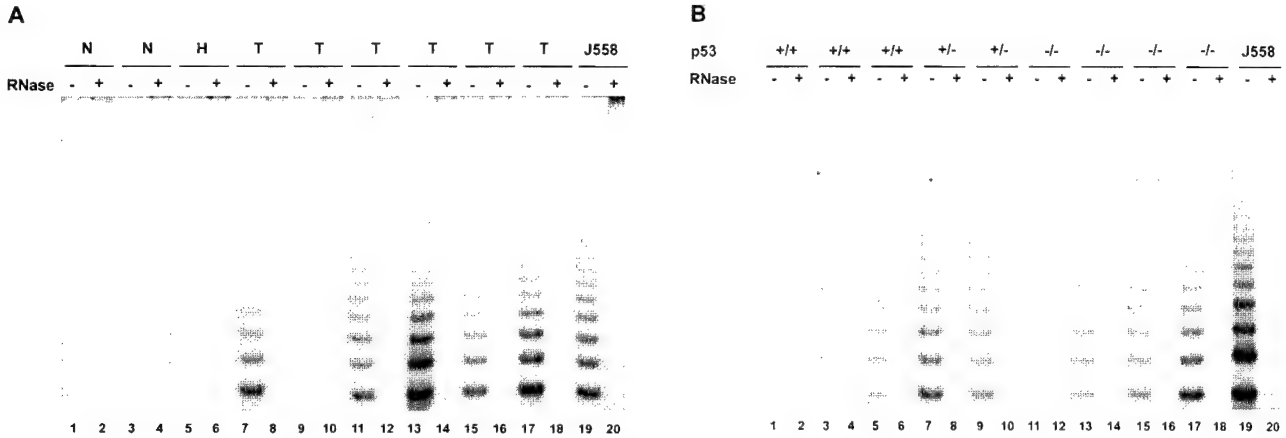

FIG. 2. Telomerase activity in normal and hyperplastic mammary glands and in mammary tumors. Telomerase activity was determined in tissue extracts by a modified version of the TRAP assay (see Materials and Methods for details) and 0.2 to 0.8 μg of protein. The murine myeloma cell line J558 is assayed in parallel as a standard (lanes 19 and 20). (A) Telomerase activity in normal SJL mammary glands (N, lanes 1 to 4), *Wnt-1* transgenic hyperplastic mammary glands (H, lanes 5 and 6), and *Wnt-1* transgenic mammary carcinomas (T, lanes 7 to 18). (B) Telomerase activity in *Wnt-1*-induced mammary tumors from mice with different *p53* genotypes. Lanes 1 to 18 contain TRAP products obtained with mammary tumor extracts. The genotype of the mice carrying the tumors is indicated above the lanes. Even-numbered lanes in both panels contain TRAP products obtained with extracts that are treated with RNase A.

TABLE 1. Activation of telomerase in Wnt-1 TG mammary tumors

Type and designation of sample	Telomerase activity[a]
Normal mammary gland	
MG 2B	4.4 (2)
MG 4B	7.6 (2)
MG 5B	2.7 (2)
MG 6B	5.9 (2)
MG 7B	1.2 (2)
MG 8B	3.0 (2)
MG 10B	1.5 (2)
MG 1-1	1.6 (2)
MG 2	5.6 (2)
MG 4	3.9 (3)
MG 2200	7.8 (2)
MG 2300	2.5 (3)
Median	3.1 (n = 12)
Hyperplastic mammary gland	
hMG 2	3.1 (2)
hMG 3	13.8 (4)
hMG 4	3.0 (2)
hMG 11	2.1 (2)
hMG 14	1.8 (2)
hMG K4	11.6 (3)
hMG 1328	9.5 (3)
hMG 1546	2.1 (2)
Median	3.1 (n = 8)
Mammary tumor	
MT 1	51 (4)
MT 2	43 (5)
MT 3	33 (2)
MT 4	5 (3)
MT 5	45 (5)
MT 6	30 (2)
MT 15B	59 (3)
MT 16B	89 (2)
MT 17B	34 (2)
MT 18B	63 (3)
MT K4	357 (2)
MT 1328	73 (5)
MT 1329	59 (3)
MT 1563	56 (2)
Median	54 (n = 14)

[a] Telomerase activity is expressed as relative specific activity normalized to a mouse J558 standard. Average percent activity was determined from two to five assays as indicated in parentheses for each sample.

utable to telomerase. As an additional control, duplicate extracts were prepared from 12 mammary tissue samples and found to give reproducible results (data not shown). It should be noted, however, that these methods do not control for possible variations in nuclease and protease activities, which could potentially reduce the recovery of active telomerase in the extracts.

Quantitative analysis indicated that the telomerase activity in normal and *Wnt-1* transgenic hyperplastic mammary glands was low, ranging from 1 to 14% of the J558 standard (Table 1). The median values for 12 normal mammary glands and 8 hyperplastic glands were identical (3.1%) (Table 1). In comparison with the normal and hyperplastic glands, the telomerase activity was significantly elevated in the *Wnt-1* transgenic mammary tumors (Fig. 2A and Table 1). The majority (13 of 14) of the tumors had telomerase levels that were greater than 30% of the standard (Table 1), and the median specific activity was 54%, which is 10- to 20-fold higher than in the nonmalignant tissues (Table 1). These data indicate that telomerase is upregulated in the majority of the *Wnt-1*-induced mouse mammary carcinomas and that this upregulation occurs at a stage after the formation of hyperplastic tissues. Elevated telomerase activity has also been documented in human breast carcinoma (30, 34).

Telomerase activation in p53-deficient mice. Telomerase activity was detectable by TRAP assay in all tested normal mammary glands from p53-deficient mice, in malignant mammary glands from *Wnt-1* transgenic mice lacking a functional *p53* gene, and in tumors arising in *p53* heterozygous mice carrying the *Wnt-1* transgene (Fig. 2A and Table 2). Normal mammary gland samples from $p53^{-/-}$ animals not carrying the *Wnt-1* transgene were assayed and revealed a low basal level of telomerase (approximately 9.3% [Table 2]). Similar to what was observed in mice with functional *p53* genes, the telomerase activity in the p53-deficient mice is consistently elevated in the *Wnt-1*-induced mammary tumors (Table 2). These results indicate that p53 function is not required for the suppression of telomerase in normal tissues or for the upregulation of the enzyme activity during mouse mammary tumorigenesis.

The *Wnt-1* transgenic/p53-deficient animals used in this study were derived from crosses of SJL mice carrying the *Wnt-1* transgene to 129/Sv mice lacking a functional *p53* gene. The resulting F_2 litters also contained *Wnt-1* transgenic animals with a $p53^{+/+}$ genotype. The telomerase activity in *Wnt-1*-induced tumors from five such $p53^{+/+}$ mice was approximately twofold lower than that in tumors from their $p53^{-/-}$ littermates (24 versus 54% [Table 2]), suggesting a subtle effect of *p53* status on the activation of telomerase. However, the tumor telomerase levels in the $p53^{+/+}$ animals from this cross are also approximately twofold lower than the telomerase activity in *Wnt-1*-induced tumors in SJL mice (24 versus 54%; compare Tables 1 and 2). Since SJL mice have functional *p53* genes, this difference would suggest a strain-specific variation in the level of telomerase upregulation during mammary tumorigenesis. Further analysis is required to confirm these minor effects of genetic background and *p53* status on the regulation of telomerase.

Correlation between telomerase RNA and histone H4 mRNA. Changes in the steady-state levels of the 430-nt mouse telomerase RNA (mTR) (7) were determined by RNA blotting in 6 normal mammary glands, 3 hyperplastic glands, and 11 tumors (Fig. 3A). The mTR signal was normalized to the signal obtained with probes for 7SK, a highly abundant and stable RNA polymerase III transcript that is expressed at the same level in normal and transformed mouse cells (11). Normalization of the mTR signals to the RNA component of RNase P gave the same results (data not shown). Telomerase template levels were similar in the normal and hyperplastic mammary glands and were elevated in the tumors, consistent with the increased telomerase activity in the mammary carcinomas (see Table 3). Upregulation of mTR did not appear to be affected by the *p53* status of the animals. Although both the telomerase activity and the mTR levels are enhanced in the tumors, linear regression analysis indicated that there was no direct correlation between the enzymatic activity and the abundance of the telomerase RNA in individual samples (Table 3). In addition, the data indicate that the enzymatic activity is upregulated more strongly (10-fold) during tumorigenesis than the telomerase RNA (2-fold) (Table 3), suggesting that the activation of telomerase involves multiple levels of regulation. Differential regulation of telomerase activity and telomerase RNA has also recently been noted in mouse skin and pancreatic islet tumors (8).

TABLE 2. Activation of telomerase in Wnt-1 TG mammary tumors in mice with different p53 genotypes

Type and designation of sample	Telomerase activity[a]
$p53^{-/-}$ normal mammary gland	
MG $1^{-/-}$	9.3 (6)
MG $2^{-/-}$	4.5 (2)
MG $3^{-/-}$	18.3 (5)
Median	9.3 ($n = 3$)
$p53^{+/+}$ mammary tumor	
W2	17 (3)
W10	11 (2)
W30	36 (3)
W134	54 (3)
W151	24 (3)
Median	24 ($n = 5$)
$p53^{-/-}$ mammary tumor	
W98	100 (3)
W121	94 (2)
W154	56 (3)
W177	14 (3)
W184	55 (4)
Median	54 ($n = 5$)

[a] Telomerase activity is expressed as relative specific activity normalized to a mouse J558 standard. Average percent activity was determined from two to six assays as indicated in parentheses for each sample.

TABLE 3. Comparison of levels of telomerase RNA, histone H4 mRNA, and telomerase activity

Sample[a]	mTR[b]	H4 mRNA[b]	Telomerase[c]
Normal and hyperplastic mammary gland[e]			
MG 2	0.29	0.50	5.6
MG 4	0.46	0.36	3.9
MG2200	0.49	0.97	7.8
MG $1^{-/-}$	0.21	0.78	9.3
MG $2^{-/-}$	0.42	0.78	4.5
MG $3^{-/-}$	0.75	1.5	18
hMG 1328	0.45	0.42	9.5
hMG 1546	0.31	0.72	2.1
hMG K4	0.31	0.61	12
Median	0.45	0.61	7.8
Mammary tumor[d]			
MT 1328	1.0	1.0	73
MT 1329	0.56	0.48	59
MT 1563	1.3	2.3	56
MT K4	1.2	1.5	357
W2	0.99	1.3	17
W10	0.49	0.48	11
W134	0.98	1.2	54
W151	0.31	0.54	24
W98	0.60	1.3	100
W154	1.2	1.3	56
W177	0.66	0.80	14
Median	0.98	1.1	56

[a] For genotypes of the mice from which these samples are derived, see Tables 1 and 2.
[b] Telomerase template RNA (mTR) and histone H4 mRNA levels were normalized to 7SK RNA (see legend to Fig. 3).
[c] Relative specific telomerase activities (see Tables 1 and 2).
[d] On the basis of Student's t test, the mTR, H4 mRNA, and telomerase activity levels are significantly increased in the tumor samples ($P < 0.001$).

The steady-state level of telomerase RNA showed a close correlation with histone H4 mRNA (Fig. 3 and Table 3), a marker for cell proliferation. Histone H4 mRNA is specifically expressed in proliferating cells, with the peak levels occurring in S phase (reviewed in reference 59). The observed correlation between H4 mRNA and mTR is not simply a consequence of elevated expression of both markers during tumorigenesis. The tumors showed a wide range of histone H4 mRNA levels, and the mTR levels in these samples fluctuated in concert (Fig. 3B). Thus, the correlation of mTR and H4 mRNA suggests that the RNA component of telomerase is upregulated in response to proliferation. Our data are consistent with a regulation of the telomerase activity that involves both induction of the telomerase RNA with cell proliferation and an additional event(s) that affects other components of the enzyme.

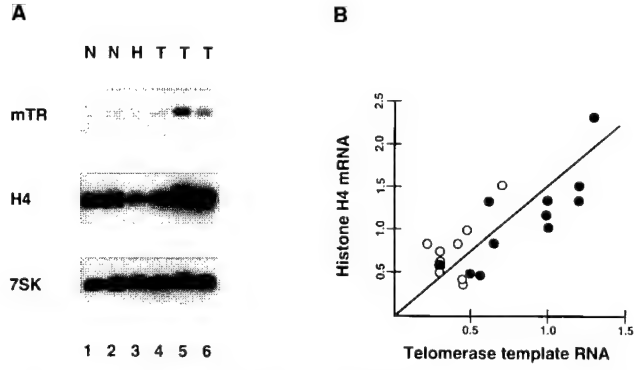

FIG. 3. Correlation of telomerase template RNA with histone H4 mRNA. (A) Total RNA from normal mammary glands (N, lanes 1 and 2), a hyperplastic mammary gland from a *Wnt-1* transgenic mouse (H, lane 3), and three *Wnt-1* transgenic mammary tumors (T, lanes 4 to 6) was blotted and sequentially probed for the 430-nt telomerase RNA (mTR), the ~400-nt histone H4 mRNA (H4), and the 330-nt 7SK RNA (7SK). (B) Relationship between the normalized levels of mTR and histone H4 mRNA in normal and hyperplastic mammary glands (open circles) and mammary tumors (filled circles). Steady-state levels of H4 mRNA and mTR were quantitated from RNA blots similar to the blot shown in panel A and normalized to 7SK RNA (Table 3). The expression levels on each axis are given in arbitrary units. Linear regression analysis indicates that mTR and histone H4 mRNA are closely correlated ($P < 0.0001$).

DISCUSSION

Mechanism of telomerase activation in mouse tumors. The work presented here aimed to test the link between telomere attrition and activation of telomerase during tumorigenesis. To address this issue, we focused on tumorigenesis in *M. musculus*. This animal has extraordinarily long telomeres in its somatic tissues, estimated to contain TTAGGG repeat arrays in excess of 20 kb, which should allow for considerable expansion of malignant cell populations without activation of telomere maintenance functions. Analysis of telomeres in transgenic animals confirmed the presence of long telomeric repeat arrays and indicated no detectable reduction in telomere length in mammary tumors induced by a mouse mammary tumor virus long terminal repeat-driven *Wnt-1* transgene. On the basis of our data, general telomere attrition does not appear to constitute a proliferative hurdle in these tumors. Nevertheless, the

RNA component and the activity of telomerase were clearly elevated during the formation of mammary carcinomas. A recent report similarly documented activation of telomerase in mouse skin carcinomas and in pancreatic islet tumors (8).

Our data demonstrate a strong correlation ($P < 0.0001$) between the expression of telomerase RNA and histone H4 mRNA, a marker for cell proliferation. This result suggests that at least one component of telomerase, its template RNA, is expressed at higher levels in cells that are actively progressing through the cell cycle. The correlation between mTR expression and cell proliferation is corroborated by immunostaining for proliferation cell nuclear antigen, a factor associated with DNA polymerase δ. Consistent with the twofold increase in H4 mRNA and telomerase RNA, the frequency of proliferating cell nuclear antigen-positive nuclei was elevated two- to threefold in tumors compared with hyperplastic mammary glands (33). The connection between telomerase RNA and cell proliferation is also consistent with the higher levels of mTR in newborn versus adult mouse tissues and the increased expression of mTR in immortalized fibroblasts (7). Whether telomerase RNA is actually induced in S phase or upregulated during the G_0-to-G_1 transition remains to be determined. In favor of the latter possibility, previous analysis showed that telomerase activity is present throughout the cell cycle of *Xenopus* eggs (44) and a number of mammalian cells (25). We note that the hyperplastic mammary glands do not appear to express more mTR, histone H4 mRNA, and telomerase activity than normal mammary glands. The lack of telomerase activation and proliferation in these tissues is consistent with the differentiated histology of hyperplastic mammary glands and their relatively low levels of proliferating cell nuclear antigen-cdk2 complexes and other parameters of cycling cells (52).

In addition to upregulation of telomerase RNA with cell proliferation, our data suggest that the tumor-specific activation of telomerase is regulated at a second level. While telomerase RNA was increased twofold in the tumors, their telomerase activity was 10-fold higher than in nonmalignant tissues. The target of this second regulatory mechanism could be a protein component of the enzyme or a telomerase inhibitor. Elucidation of this issue awaits cloning of the protein components of telomerase. We note that our data do not exclude that this level of regulation is also linked to the proliferative state of the cells. Telomerase activity is upregulated upon mitogenic stimulation of human peripheral blood lymphocytes (31), increased during in vitro culturing of primary mouse cells (12), and repressed during terminal differentiation of human and mouse cell lines (56). However, in a number of studies the correlation of telomerase activity with proliferation is less clear (16, 17, 34), suggesting additional levels of regulation or cell-type-dependent regulatory pathways. Multiple levels of telomerase regulation are compatible with findings with *Saccharomyces cerevisiae* in which a large number of genes affect telomere dynamics (reviewed in reference 64).

Telomerase function. It is not clear what role telomerase fulfills in proliferating *M. musculus* cells. If the enzyme is needed to maintain telomeres at a 20- to 50-kb length, this raises the question of why *M. musculus* requires telomeres that are approximately 10-fold longer than the 1- to 2-kb telomeres that appear fully functional in some human and mouse cells (4, 15, 16, 53). Another possibility is that telomerase activity is required in proliferating cells to add a 3′ overhang to the blunt ends created by leading strand synthesis (42). However, in two budding yeasts loss of telomerase activity through inactivation of their telomerase RNA genes does not diminish short-term cell viability (46, 57), suggesting that 3′ telomere termini are either not required or can be generated by another mechanism. Another, as yet unexplored, possibility is that a telomerase protein is required as a structural component of the telomeric complex (9, 20).

While a structural role for telomerase at telomeres is in keeping with the moderate upregulation of telomerase RNA in proliferating cells, it does not explain the 10- to 20-fold increase in telomerase activity observed in tumors. Since there is no demonstrable telomere shortening during tumorigenesis, it is unlikely that telomerase activation functions to counter gross telomeric decline. However, as discussed below, it is possible that the genomic blots failed to detect one or more shortening "clock telomeres" that require activated telomerase for their maintenance. A second possibility is that the activated tumor telomerase serves to heal damaged chromosomes.

Structure of mouse telomeres. It is pertinent to this study to consider what is known about telomere structure in *M. musculus*. An important assumption in our interpretation of the findings is that all telomeres of this species end in long uninterrupted stretches of precise TTAGGG repeats. This view is consistent with the absence of restriction endonuclease cleavage sites in the terminal 20 to 50 kb, with the strong hybridization of mouse telomeres to telomeric sequences, and with the presence of TTAGGG repeats on terminal fragments that have been shortened by ~20 kb through digestion with exonuclease BAL 31 (37, 58). Is it possible that one or more of these telomeres have a different structure? For instance, if one of the chromosome ends carries a much shorter telomeric stretch, the decline of this telomere could drive telomerase activation during tumorigenesis. Quantitative in situ detection methods will be required to establish whether normal *M. musculus* cells harbor such clock telomeres.

We have also considered the possibility that *M. musculus* chromosomes might have long subtelomeric regions of TTA GGG-related repeats, similar to the blend of variant repeats found at the base of human telomeres (2, 10). Such sequences would explain the absence of restriction endonuclease recognition sites and the strong hybridization of the terminal fragments to TTAGGG repeat probes. Yet, these repeats would probably not function to protect chromosome ends. For instance, the mammalian telomeric protein TRF fails to bind these sequences (13, 65), and de novo formation of telomeres requires precise TTAGGG repeats (27). A frequently occurring variant in the subtelomeric TTAGGG-related repeats has a T→G transversion (TGAGGG) (10), introducing *Mn*II (GAGG) and *Hph*I (GGGTGA) recognition sites in the arrays. Indeed, these enzymes remove about 2 kb from human terminal restriction fragments, consistent with the estimates for the region of mixed repeats at the base of human telomeres (2). Yet, both *Mn*II and *Hph*I yield telomeric fragments in *M. musculus* that are larger than 20 kb (35, 58), arguing against extensive degenerate telomeric arrays in these telomeres. Thus, the available evidence is consistent with the presence of exceedingly long stretches of tandem TTAGGG repeats at *M. musculus* chromosome ends.

p53 and telomere dynamics. Two main conclusions can be drawn from the analysis of mice lacking a functional *p53* gene. First, with regard to telomere dynamics and telomerase regulation, these mice were very similar to the transgenic mice with functional *p53* genes. Although minor regulatory changes cannot be excluded, we tentatively conclude that the induction of mTR with cell proliferation and the activation of telomerase during tumorigenesis do not require p53 function. During immortalization of human cells, telomerase activation is also independent of p53 function (62). Second, our results are pertinent to the genomic instability observed in mammary tumors

originating in p53-deficient mice (22). The chromosomal abnormalities seen in these tumor cells include numerical changes, amplifications, and dicentrics, which are associated with telomere shortening in human cells (reviewed in reference 20). However, our results fail to reveal significant telomere shortening in the *Wnt-1* transgenic $p53^{-/-}$ mammary tumors, suggesting that the genome instability in these $p53^{-/-}$ tumors is not due to loss of telomeric DNA.

Comparison of murine and human telomeres. Telomere dynamics in mice and humans differ. Our results show that the bulk of the telomeres do not shorten significantly during mouse tumorigenesis. Therefore, it is unlikely that the telomere-dependent tumor suppressor mechanism proposed for human cells functions as such in mice. However, in other aspects telomere metabolism in murine and human cells may be more similar. Specifically, the regulation of telomerase in normal and tumor tissues appears comparable in both systems. In mice and humans, telomerase RNA can be detected in somatic cells, and in both systems, the enzyme is consistently activated in tumors. These parallels suggest that insights in telomere dynamics and telomerase regulation in mice may bear on the role of telomerase in human cancer.

ACKNOWLEDGMENTS

We are indebted to Nam Kim and Calvin Harley (Geron Corp., Menlo Park, Calif.), Howard Cooke and David Kipling (MRC, Edinburgh, United Kingdom), and Jerry Shay (University of Texas at Dallas) for providing us with unpublished information and protocols. David Kipling is also thanked for extensive discussion of this work. We thank Richard Lang (New York University) for help with PhosphorImager analysis and comments on the manuscript and Neil Segil and Steve Schiff (The Rockefeller University) for advice on cell cycle issues. Carol Greider (Cold Spring Harbor Laboratory) and Nat Heintz (The Rockefeller University) are thanked for providing us with the mTR and H4 plasmids, respectively. Art Lustig (Memorial Sloan Kettering Cancer Center) and members of the de Lange laboratory are thanked for comments on the manuscript.

This work was supported by grants from the Irma T. Hirschl Foundation, the Rita Allen Foundation, and the NIH (GM49046) to T.D.L. and by a grant from the DOD Breast Cancer Program to L.A.D. D.B. is the recipient of a Merck Fellowship.

REFERENCES

1. **Allshire, R. C., G. Cranston, J. R. Gosden, J. C. Maule, N. D. Hastie, and P. A. Fantes.** 1987. A fission yeast chromosome can replicate autonomously in mouse cells. Cell **50:**391–403.
2. **Allshire, R. C., M. Dempster, and N. D. Hastie.** 1989. Human telomeres contain at least three types of G-rich repeats distributed non-randomly. Nucleic Acids Res. **17:**4611–4627.
3. **Allshire, R. C., J. R. Gosden, S. H. Cross, G. Cranston, D. Rout, N. Sugawara, J. W. Szostak, P. A. Fantes, and N. D. Hastie.** 1988. Telomeric repeat from T. thermophila cross-hybridizes with human telomeres. Nature (London) **332:**656–659.
4. **Allsop, R. C., and C. B. Harley.** 1995. Evidence for a critical telomere length in senescent human fibroblasts. Exp. Cell Res. **219:**130–136.
5. **Auffray, C., and G. Rougeon.** 1980. Purification of mouse immunoglobulin heavy-chain messenger RNAs from total myeloma tumor RNA. Eur. J. Biochem. **107:**303–314.
6. **Blackburn, E. H.** 1993. Telomerase, p. 557–576. *In* R. F. Gesteland and J. F. Atkins (ed.), The RNA world. Cold Spring Harbor Laboratory Press, Cold Spring Harbor, N.Y.
7. **Blasco, M. A., W. Funk, B. Villeponteau, and C. W. Greider.** 1995. Functional characterization and developmental regulation of mouse telomerase RNA. Science **269:**1267–1270.
8. **Blasco, M. A., M. Rizen, C. W. Greider, and D. Hanahan.** 1996. Differential regulation of telomerase activity and telomerase RNA during multi-stage tumorigenesis. Nature (London) Genet. **12:**200–204.
9. **Broccoli, D., J. W. Young, and T. de Lange.** 1995. Telomerase activity in normal and malignant hematopoietic cells. Proc. Natl. Acad. Sci. USA **92:** 9082–9086.
10. **Brown, W. R. A., P. J. MacKinnon, A. Villasante, N. Spurr, V. J. Buckle, and M. J. Dobson.** 1990. Structure and polymorphism of human telomere-associated DNA. Cell **63:**119–132.
11. **Carey, M. F., K. Singh, M. Botchan, and N. R. Cozzarelli.** 1986. Induction of specific transcription by RNA polymerase III in transformed cells. Mol. Cell. Biol. **6:**3068–3076.
12. **Chadeneau, C., P. Siegel, C. B. Harley, J. W. Muller, and S. Bacchetti.** 1995. Telomerase activity in normal and malignant murine tissues. Oncogene **11:** 893–898.
13. **Chong, L., B. van Steensel, D. Broccoli, H. Erdjument-Bromage, J. Hanish, P. Tempst, and T. de Lange.** 1995. A human telomeric protein. Science **270:**1663–1667.
14. **Church, G. M., and W. Gilbert.** 1984. Genomic sequencing. Proc. Natl. Acad. Sci. USA **81:**1991–1995.
15. **Cooke, H., and D. Kipling.** Personal communication.
16. **Counter, C. M., A. A. Avilion, C. E. LeFeuvre, N. G. Stewart, C. W. Greider, C. B. Harley, and S. Bacchetti.** 1992. Telomere shortening associated with chromosome instability is arrested in immortal cells with express telomerase activity. EMBO J. **11:**1921–1929.
17. **Counter, C. M., F. M. Botelho, P. Wang, C. B. Harley, and S. Bacchetti.** 1994. Stabilization of short telomeres and telomerase activity accompany immortalization of Epstein-Barr virus-transformed human B lymphocytes. J. Virol. **68:**3410–3414.
18. **Counter, C. M., J. Gupta, C. B. Harley, B. Lever, and S. Bacchetti.** 1995. Telomerase activity in normal leukocytes and in haematological malignancies. Blood **85:**2315–2320.
19. **Counter, C. M., H. W. Hirte, S. Bacchetti, and C. Harley.** 1994. Telomerase activity in human ovarian carcinoma. Proc. Natl. Acad. Sci. USA **91:**2900–2904.
20. **de Lange, T.** 1995. Telomere dynamics and genome instability in human cancer, p. 265–295. *In* E. H. Blackburn and C. W. Greider (ed.), Telomeres. Cold Spring Harbor Laboratory Press, Cold Spring Harbor, N.Y.
21. **de Lange, T., L. Shiue, R. M. Myers, D. R. Cox, S. L. Naylor, A. M. Killery, and H. E. Varmus.** 1990. Structure and variability of human chromosome ends. Mol. Cell. Biol. **10:**518–527.
22. **Donehower, L. A., L. A. Godley, C. M. Aldaz, R. Pule, Y.-P. Shi, D. Pinkel, J. Gray, A. Bradley, D. Median, and H. E. Varmus.** 1995. Deficiency of p53 accelerates mammary tumorigenesis in Wnt-1 transgenic mice and promotes chromosomal instability. Genes Dev. **9:**882–895.
23. **Feng, J., W. D. Funk, S.-S. Wang, S. L. Weinrich, A. A. Avilion, C.-P. Chiu, R. R. Adams, E. Chang, R. C. Allsopp, J. Yu, S. Le, M. D. West, C. B. Harley, W. H. Andrews, C. W. Greider, and B. Villeponteau.** 1995. The RNA component of human telomerase. Science **269:**1236–1241.
24. **Garagna, S., D. Broccoli, C. A. Redi, J. B. Searle, H. J. Cooke, and E. Capanna.** 1995. Robertsonian metacentrics of the house mouse lose telomeric sequences but retain some minor satellite DNA in the pericentromeric area. Chromosoma **103:**685–692.
25. **Greider, C. W.** 1995. Telomerase biochemistry and regulation, p. 35–69. *In* E. H. Blackburn and C. W. Greider (ed.), Telomeres. Cold Spring Harbor Laboratory Press, Cold Spring Harbor, N.Y.
26. **Greider, C. W., and E. H. Blackburn.** 1985. Identification of a specific telomere terminal transferase activity in Tetrahymena extracts. Cell **43:**405–413.
27. **Hanish, J. P., J. Yanowitz, and T. de Lange.** 1994. Stringent sequence requirements for telomere formation in human cells. Proc. Natl. Acad. Sci. USA **91:**8861–8865.
28. **Harley, C. B., A. B. Futcher, and C. W. Greider.** 1990. Telomeres shorten during ageing of human fibroblasts. Nature (London) **345:**458–460.
29. **Harley, C. B., and B. Villeponteau.** 1995. Telomere and telomerase in aging and cancer. Curr. Opin. Genet. Dev. **5:**249–255.
30. **Hiyama, E., L. Gollahan, T. Karaoka, K. Kuroi, T. Yokoyama, A. F. Gazdar, K. Hiyama, M. A. Piatyszek, and J. W. Shay.** 1996. Telomerase activity in human breast tumors. J. Natl. Cancer Inst. **88:**116–122.
31. **Hiyama, K., Y. Hirai, S. Kyoizumi, M. Akiyama, E. Hiyama, M. A. Piatsyszek, J. W. Shay, S. Ishioka, and M. Ymakido.** 1995. Activation of telomerase in human lymphocytes and hematopoietic progenitor cells. J. Immunol. **155:**3711–3715.
32. **Ishikawa, F., M. J. Matunis, G. Dreyfuss, and T. R. Cech.** 1993. Nuclear proteins that bind the pre-mRNA 3′ splice site sequence r(UUAG/G) and the human telomeric DNA sequence $d(TTAGGG)_n$. Mol. Cell. Biol. **13:** 4301–4310.
33. **Jones, J., and L. A. Donehower.** Unpublished observation.
34. **Kim, N. W., M. A. Piatyszek, K. R. Prowse, C. B. Harley, M. D. West, P. L. C. Ho, G. M. Coviello, W. E. Wright, S. L. Weinrich, and J. W. Shay.** 1994. Specific association of human telomerase activity with immortal cells and cancer. Science **266:**2011–2015.
35. **Kipling, D.** Personal communication.
36. **Kipling, D., H. E. Ackford, A. R. Mitchell, B. A. Taylor, and H. J. Cooke.** 1991. Mouse minor satellite DNA genetically maps to the centromere and is physically linked to the proximal telomere. Genomics **11:**235–241.
37. **Kipling, D., and H. J. Cooke.** 1990. Hypervariable ultra-long telomeres in mice. Nature (London) **347:**347–402.
38. **Kipling, D., H. E. Wilson, E. J. Thomson, and H. J. Cooke.** 1995. YAC cloning Mus musculus telomeric DNA: physical, genetic, in situ and STS markers for the distal telomere of chromosome 10. Hum. Mol. Genet. **4:**1007–1014.

39. **Klingelhutz, A. J., S. A. Barber, P. Smith, K. Dyer, and J. K. McDougall.** 1994. Restoration of telomeres in human papillomavirus-immortalized human anogenital epithelial cells. Mol. Cell. Biol. **14:**961–969.
40. **Kramer, K., and J. Haber.** 1993. New telomeres in yeast are initiated with a highly selected subset of TG_{1-3} repeats. Genes Dev. **7:**2345–2356.
41. **Kwan, H., V. Pecenka, A. Tsukamoto, T. G. Parslow, R. Guzman, T.-P. Lin, W. J. Muller, F. S. Lee, P. Leder, and H. E. Varmus.** 1992. Transgenes expressing Wnt-1 and int-2 proto-oncogenes cooperate during mammary carcinogenesis in doubly transgenic mice. Mol. Cell. Biol. **12:**147–154.
42. **Lingner, J., J. P. Cooper, and T. R. Cech.** 1995. Telomerase and DNA end replication: no longer a lagging strand problem? Science **269:**1533–1534.
43. **MacArthur, C. A., D. B. Shankar, and G. M. Shackleford.** 1995. Fgf-8, activated by proviral insertion, cooperates with the Wnt-1 transgene in murine mammary tumorigenesis. J. Virol. **69:**2501–2507.
44. **Mantell, L. L., and C. W. Greider.** 1994. Telomerase activity in germline and embryonic cells of Xenopus. EMBO J. **13:**3211–3217.
45. **McClintock, B.** 1941. The stability of broken ends of chromosomes in zea mays. Genetics **26:**234–282.
46. **McEachern, M. J., and E. H. Blackburn.** 1995. Runaway telomere elongation caused by telomerase RNA gene mutations. Nature (London) **376:**403–409.
47. **Meyne, J., R. J. Baker, H. H. Hobart, T. C. Hsu, O. A. Ryder, O. G. Ward, J. E. Wiley, D. H. Wurster-Hill, T. L. Yates, and R. K. Moyzis.** 1990. Distribution of non-telomeric sites of the (TTAGGG)n telomeric sequence in vertebrate chromosomes. Chromosoma **99:**3–10.
48. **Moon, I. S., and M. O. Kraus.** 1991. Common RNA polymerase I, II, and III upstream elements in mouse 7SK gene locus revealed by the inverse polymerase chain reaction. DNA Cell Biol. **10:**23–32.
49. **Morin, G. B.** 1989. The human telomere terminal transferase enzyme is a ribonucleoprotein that synthesizes TTAGGG repeats. Cell **59:**521–529.
50. **Prowse, K., A. Avilion, and C. Greider.** 1993. Identification of a nonprocessive telomerase activity from mouse cells. Proc. Natl. Acad. Sci. USA **90:**1493–1497.
51. **Prowse, K., and C. W. Greider.** 1995. Developmental and tissue specific regulation of mouse telomerase and telomere length. Proc. Natl. Acad. Sci. USA **92:**4818–4822.
52. **Said, T. K., and D. Medina.** 1995. Cell cyclins and cyclin-dependent kinase activities in mouse mammary tumor development. Carcinogenesis **16:**823–830.
53. **Saltman, D., R. Morgan, M. L. Cleary, and T. de Lange.** 1993. Telomeric structure in cells with chromosome end associations. Chromosoma **102:**121–128.
54. **Sandell, L., and V. Zakian.** 1993. Loss of a yeast telomere: arrest, recovery, and chromosome loss. Cell **75:**729–741.
55. **Shackleford, G. M., C. A. MacArthur, H. C. Kwan, and H. E. Varmus.** 1993. Mouse mammary tumor virus infection accelerates mammary carcinogenesis in Wnt-1 transgenic mice by insertional activation of int-2/Fgf-3 and hst/Fgf-4. Proc. Natl. Acad. Sci. USA **90:**740–744.
56. **Sharma, H. W., J. A. Sokoloski, J. R. Perez, J. Y. Maltese, A. C. Sartorelli, C. A. Stein, G. Nichols, Z. Khaled, N. T. Telang, and R. Narayanan.** 1995. Differentiation of immortal cells inhibits telomerase activity. Proc. Natl. Acad. Sci. USA **92:**12343–12346.
57. **Singer, M. S., and D. E. Gottschling.** 1994. TLC1: template RNA component of Saccharomyces cerevisiae telomerase. Science **266:**404–409.
58. **Starling, J. A., J. Maule, N. D. Hastie, and R. C. Allshire.** 1990. Extensive telomere repeat arrays in mouse are hypervariable. Nucleic Acids Res. **18:**6881–6888.
59. **Stein, G. S., J. L. Stein, A. J. van Wijnen, and J. B. Lian.** 1992. Regulation of histone gene expression. Curr. Opin. Cell Biol. **4:**166–173.
60. **Tsukamoto, A. S., R. Grosschedl, R. C. Guzman, T. Parslow, and H. E. Varmus.** 1988. Expression of the int-1 gene in transgenic mice is associated with mammary gland hyperplasia and adenocarcinomas in male and female mice. Cell **55:**619–625.
61. **Watson, J. D.** 1972. Origin of concatemeric T7 DNA. Nature (London) **239:**197–201.
62. **Whitaker, N. J., T. M. Bryan, P. Bonnefin, A. C.-M. Chang, E. A. Musgrove, A. W. Braithwaite, and R. R. Reddel.** 1995. Involvement of RB-1, p53, p16INK4, and telomerase in immortalisation of human cells. Oncogene **11:**971–976.
63. **Wright, W. E., J. W. Shay, and M. A. Piatyszek.** 1995. Modifications of a telomeric repeat amplification protocol (TRAP) result in increased reliability, linearity and sensitivity. Nucleic Acids Res. **23:**3794–3795.
64. **Zakian, V. A.** 1995. Saccharomyces telomeres: function, structure and replication, p. 107–138. *In* E. H. Blackburn and C. W. Greider (ed.), Telomeres. Cold Spring Harbor Laboratory Press, Cold Spring Harbor, N.Y.
65. **Zhong, Z., L. Shiue, S. Kaplan, and T. de Lange.** 1992. A mammalian factor that binds telomeric TTAGGG repeats in vitro. Mol. Cell. Biol. **13:**4834–4843.

Genetics and Cancer Susceptibility:
Implications for Risk Assessment, pages 1–11

THE ROLE OF p53 LOSS IN GENOMIC INSTABILITY AND TUMOR PROGRESSION IN A MURINE MAMMMARY CANCER MODEL

Lawrence A. Donehower, Lucy A. Godley, C. Marcelo Aldaz, Ruth Pyle, Yu-Ping Shi, Dan Pinkel, Joe Gray, Allan Bradley, Daniel Medina, and Harold E. Varmus

Division of Molecular Virology, Baylor College of Medicine, Houston,TX 77030 ; (L.A.D., R.P.); Varmus Laboratory, National Cancer Institute, Bethesda, MD 20892 and Department of Biochemistry and Biophysics, University of California, San Francisco, CA 94143 (L.A.G.); Department of Carcinogenesis, University of Texas M.D. Anderson Cancer Center-Science Park, Smithville, TX 78957 (C.M.A.); Division of Molecular Cytometry, Department of Laboratory Medicine, University of California at San Francisco, San Francisco, CA 94143 (Y.-P.S., D.P., J.G.); Institute for Molecular Genetics and Howard Hughes Medical Institute, Baylor College of Medicine, Houston, TX 77030 (A.B); Department of Cell Biology, Baylor College of Medicine, Houston, TX 77030; (D.M.); Office of the Director, National Institutes of Health, Bethesda, MD 20892 and Department of Microbiology and Immunology, University of California, San Francisco, CA 94143 (H.E.V.)

INTRODUCTION

The p53 gene is often mutated or lost in human tumors, including about 30% of all breast cancers (Greenblatt et al., 1994). In addition, germ line mutations in the p53 gene are linked with an inherited early cancer predisposition called Li-Fraumeni syndrome (Malkin et al., 1990, Srivastava et al., 1990). The p53 gene encodes a tumor suppressor protein which can mediate G1 arrest of the cell cycle following DNA damage (Finlay et al., 1989; Kastan et al., 1992). In some contexts, p53 appears to induce apoptosis as a result of DNA damage or an intracellular imbalance in growth signals (Yonish-Rouach et al., 1991; Clarke et al., 1993; Lowe et al., 1993a). Loss of p53 in cells has been associated with a loss of cell cycle checkpoint control and increased genomic instability (Livingstone et al., 1992; Yin et al., 1992). Absence of normal p53 function in a tumor cell is correlated with a poorer clinical prognosis and a resistance to treatment with various anticancer agents (Lowe et al., 1993b; Lowe et al., 1994).

TUMORIGENESIS IN p53-DEFICIENT MICE

To investigate the role of p53 in mammalian tumorigenesis, we have utilized gene targeting techniques to generate mice with one or two disrupted germ line p53 alleles (Donehower et al., 1992). These disrupted alleles are null for p53, as they are incapable of producing intact functional p53. Over 90% of mice nullizygous for p53 (p53-/-) are developmentally normal, but are highly susceptible to early onset tumors

(Table 1). Heterozygous mice (p53+/-) were also susceptible to tumors but at a significantly delayed rate compared to the nullizygotes (Harvey et al., 1993) (Table 1). Wild type (p53+/+) littermates of the p53-deficient mice rarely developed tumors during monitoring.

Table 1. Tumorigenesis in p53-Deficient Mice[a]

Genotype	50% Tumor Incidence	Tumor Types (No. observed)	% of Total	Mean Time of Onset
p53-/-	19 weeks	Lymphomas (59)	64%	20 weeks
		Soft Tissue Sarcomas (24)	26%	21 weeks
		Osteosarcomas (2)	2%	
		Carcinomas (1)	1%	
		Other (6)	7%	
p53+/-	76 weeks	Osteosarcomas (31)	35%	66 weeks
		Lymphomas (25)	28%	64 weeks
		Soft Tissue Sarcomas (24)	27%	68 weeks
		Carcinomas (6)	7%	73 weeks
		Other (2)	2%	

[a] 92 p53-/- and 184 p53+/- mice of mixed inbred genetic background (75% C57BL/6 and 25% 129/Sv) were monitored up to two years of age.

The tumor types observed in the p53-deficient mice were predominantly lymphomas and sarcomas, with a small number of carcinomas and other tumor types (brain tumors, testicular tumors). One p53-/- and one p53+/- mouse each developed a mammary adenocarcinoma, indicating that this particular tumor type rarely occurred spontaneously.

THE EFFECTS OF p53 LOSS ON TUMORIGENESIS IN A MURINE MAMMARY CANCER MODEL

The diversity of tumor types and relatively long time to tumor onset for the p53+/- mice complicates mechanistic studies of the role of p53 in tumorigenesis. To study the role of p53 loss in tumor development in a single tissue, we crossed the p53-deficient mice to mammary tumor-susceptible *Wnt-1* transgenic mice (Tsukamoto et al., 1988). Our rationale was that the effects of the presence or absence of p53 on the development of mammary cancer could be studied more readily in the offspring of these crosses.

The *Wnt-1* transgenic (*Wnt-1 TG*) mice contain additional copies of the murine *Wnt-1* proto-oncogene adjacent to the mouse mammary tumor virus long terminal repeat

(Tsukamoto et al., 1988). This construct, when added to the mouse germ line, was shown to result in high level mammary gland expression of *Wnt-1* mRNA. Male and female mice developed hyperplastic mammary glands and ultimately mammary adenocarcinomas. Virtually all females develop carcinomas by 12 months while less than 20% of males developed this tumor by twelve months of age (Tsukamoto et al., 1988).

Following crossing of the *Wnt-1* transgenic and p53-deficient mice, twelve groups of mice (each group containing at least 16 animals) were monitored for tumor development. The parameters defining each group were sex, p53 genotype (p53+/+, p53+/-, p53-/-), and *Wnt-1* transgene status (present or absent). The mammary tumor incidence in the six categories of mice containing the *Wnt-1* transgene are shown in Tables 2A and 2B. The six groups without the *Wnt-1* transgene did not develop mammary tumors.

Table 2A. Mammary tumor incidence in p53-deficient and normal *Wnt-1* transgenic female mice

p53 Genotype	Number of animals	50% tumor incidence	100% tumor incidence	Mean tumors per mouse
p53+/+	16	22.5 weeks	40 weeks	1.17
p53+/-	32	23.0 weeks	41 weeks	1.17
p53-/-	16	11.5 weeks	15 weeks	1.28

Table 2B. Mammary tumor incidence in p53-deficient and normal *Wnt-1* transgenic male mice

p53 Genotype	Number of animals	Tumor incidence Six months	Tumor incidence Twelve months
p53+/+	21	10%	43%
p53+/-	22	20%	32%
p53-/-	12[a]	100%	

[a] Four of 16 *Wnt-1 TG* p53-/- males developed early lymphomas.

Note above that the *Wnt-1 TG* p53-/- females and males developed mammary adenocarcinomas much sooner than their *Wnt-1 TG* p53+/- and p53+/+ counterparts. The *Wnt-1*

TG p53+/- males and females did not develop tumors significantly faster than the *Wnt-1 TG* p53+/+ males and females. During tumor development, roughly half of the *Wnt-1 TG* p53+/- tumors lost their remaining wild type p53 allele, as measured by Southern blotting (data not shown). These tumors with p53 loss of heterozygosity (LOH) did not develop any sooner than those p53+/- tumors without LOH. Thus, only those animals completely lacking p53 (p53-/-) showed accelerated mammary tumor development under the influence of the *Wnt-1* transgene.

p53 LOSS AFFECTS THE HISTOPATHOLOGY OF MAMMARY ADENOCARCINOMAS

In the mammary cancer study described above, mammary tumors were recorded when the tumor reached a size of roughly 0.5 cm. When the tumor became 1.5-2.0 cm in diameter, the animal was sacrificed and histopathology performed on the tumor by standard methods. Analysis of 32 *Wnt-1 TG* p53 mammary adenocarcinomas revealed dramatic differences in the tumor histopathology which directly depended on the presence or absence of wild type p53 in the tumor. Histology of representative tumors of each p53 genotype is shown below in Fig. 1.

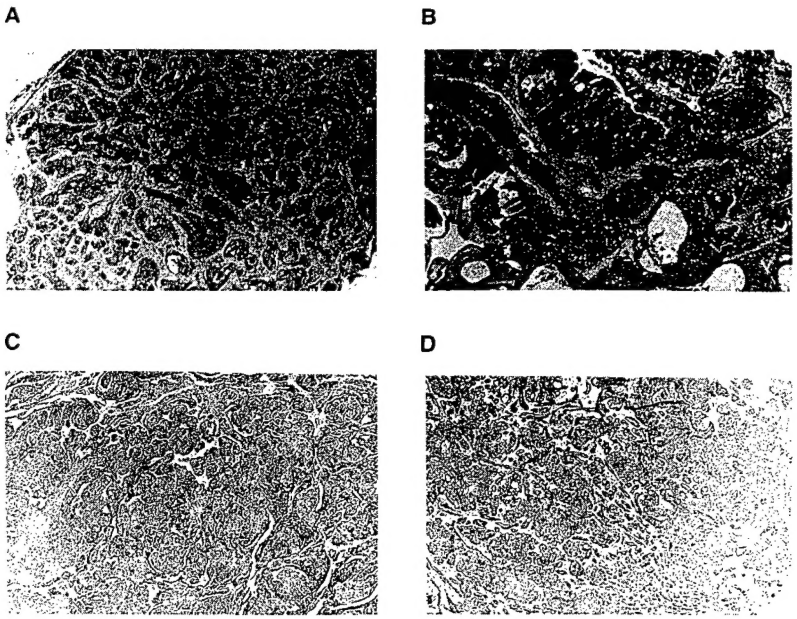

Figure 1. Histopathology of *Wnt-1 TG* p53 mammary tumors. Sections of four representative tumors were stained with hematoxylin and eosin and photographed at a magnification of 50X. (A) *Wnt-1 TG* p53+/+ tumor; (B) *Wnt-1 TG* p53+/- (no LOH) tumor; (C) *Wnt-1 TG* p53+/- (LOH) tumor; (D) *Wnt-1 TG* p53-/- tumor.

In most of those tumors which retained wild type p53 (p53+/+ and p53+/- without LOH), the tumor cells appeared more organized, with considerable stromal involvement or fibrosis. In contrast, tumors missing p53 (p53-/- or p53+/- with LOH) had much less stromal fibrosis. These tumor cells were also more anaplastic in appearance and had more mitotic figures. Table 3 shows the compilation of 32 *Wnt-1 TG* p53 female tumors analyzed by histopathology for a fibrotic or non-fibrotic appearance and their p53 genotypes.

Table 3. Histopathology of female *Wnt-1 TG* p53 tumors

p53 Genotype	With Fibrosis	Without Fibrosis
p53+/+	8 (73%)	3 (27%)
p53+/- (no LOH)	6 (75%)	2 (25%)
p53+/- (LOH)	1 (14%)	6 (86%)
p53-/-	0 (0%)	6 (100%)

Note above the strong correlation between the presence of functional wild type p53 and presence of fibrosis. The p53+/- (no LOH) tumors are believed to retain wild type p53, since the p53 cDNAs of four representative p53+/- (no LOH) tumors were sequenced and found to be wild type (data not shown). These results suggest that mammary tumorigenesis pathways in this model may be fundamentally different depending on the presence or absence of wild type p53.

EFFECTS OF p53 LOSS ON GENOMIC STABILITY IN A MAMMARY CANCER MODEL

The relatively early development of mammary tumors in the *Wnt-1 TG* p53 mice provided us with a useful model for exploring the genetic and biological effects of the presence and absence of p53 in tumor progression in a single tissue. One effect of p53 loss in tissue culture cells appears to be increased genetic instability as measured by abnormal chromosome numbers and susceptibility to gene amplification in the presence of certain drugs (Livingstone et al., 1992; Yin et al., 1992). However, we wanted to extend these observations and determine whether loss of p53 confers genetic instability in the context of an *in vivo* tumor model.

In our first set of experiments, we made cytogenetic preparations from the mammary tumor cells of p53+/+, p53+/-, and p53-/- *Wnt-1* mice to determine whether loss of p53 conferred chromosomal instability. Metaphase preparations were made according to standard procedures on tumor cells isolated 24-48 hours previously from

intact tumors (Aldaz et al., 1992). The chromosome numbers of 25-50 metaphases for 15 *Wnt-1* tumors of different p53 genotypes were determined. The results of these chromosome counts are summarized in Fig. 2.

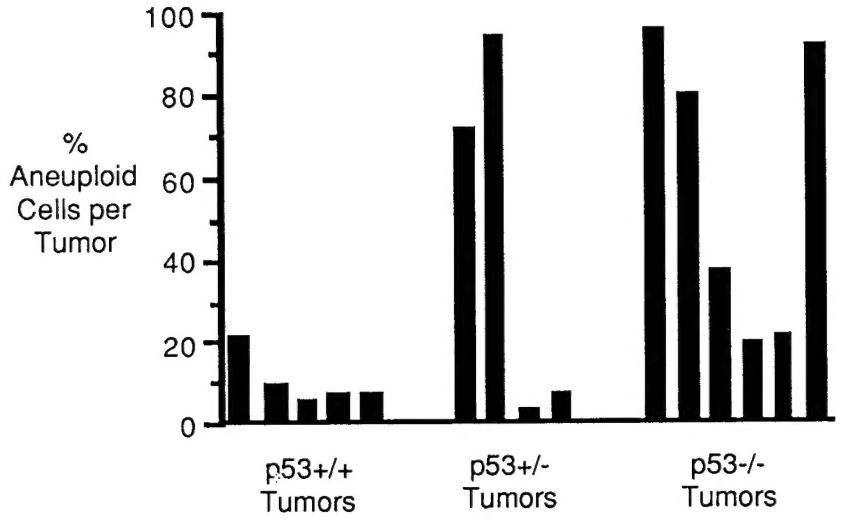

Figure. 2. Summary of cytogenetic studies in *Wnt-1 TG* p53 mice. Each tumor is represented by a bar indicating the percentage of examined cells that had chromosome numbers other than 40. The p53 genotype of each group is indicated below the graph.

Note that the great majority of cells from all of the *Wnt-1 TG* p53+/+ mammary tumors retained an apparent diploid karyotype, while several of the *Wnt-1 TG* p53-/- tumors had a high percentage of aneuploid cells. Interestingly, some of the *Wnt-1 TG* p53-/- tumors were primarily diploid in karyotype, indicating that p53 loss by itself was insufficient to confer genomic instability. The *Wnt-1 TG* p53+/- tumors displayed two patterns: one of high aneuploidy and one of apparent diploidy. When the status of the remaining wild type p53 allele in these tumors was assayed by Southern blot hybridization, both aneuploid tumors had lost the wild type allele, while in the diploid tumors, one tumor had retained the wild type allele and the second had partial loss of heterozygosity (data not shown).

The aneuploid cells in the individual *Wnt-1 TG* p53+/- and Wnt-1 p53-/- tumors tended to be heterogeneous in chromosome number. Typical tumors had high numbers of cells in the hypotetraploid range. Other tumors had a high percentage of cells missing a single chromosome (data not shown). Taken, together, these cytogenetic experiments support the concept, previously established by *in vitro* studies, that loss of p53 predisposes a developing tumor cell to chromosomal instability *in vivo*.

We employed a second type of assay, comparative genomic hybridization (CGH), to measure genomic instability in the *Wnt-1 TG* p53 tumor model. CGH detects regions of increases and decreases in DNA copy number throughout the entire genome of a tumor cell (Kallioniemi et al., 1992). This procedure was applied to 25 of our *Wnt-1 TG* p53 tumor DNAs and some of the results are shown in Table 4 and Fig. 3. First of all, the total number of chromosomal abnormalities in each tumor was partially dependent on the p53 genotype of the animal in which the tumor arose. Only two of six *Wnt-1 TG* p53+/+ tumors and two of four *Wnt-1 TG* p53+/- (no LOH) tumors exhibited chromosomal regions with DNA copy number gains or losses (Table 4). In contrast, all eight *Wnt-1 TG* p53+/- (LOH) and seven *Wnt-1 TG* p53-/- tumors displayed at least one chromosomal abnormality and many showed multiple changes in DNA copy number. As shown in Table 4, the average number of chromosomal changes per tumor was greatest in the *Wnt-1 TG* p53+/- (LOH) tumors, with an average of 4.2 abnormalities/tumor compared to 1.7 abnormalities per tumor for the *Wnt-1 TG* p53-/- tumors.

Table 4. Summary of CGH Abnormalities in the *Wnt-1 TG* p53 tumors

p53 Genotype	Tumors with Chromosome Abnormalities	Average Number of Chromosome Abnormalities per Tumor
p53+/+	2/6	0.3
p53+/- (no LOH)	2/4	1.0
p53+/- (LOH)	8/8	4.2
p53-/-	7/7	1.7

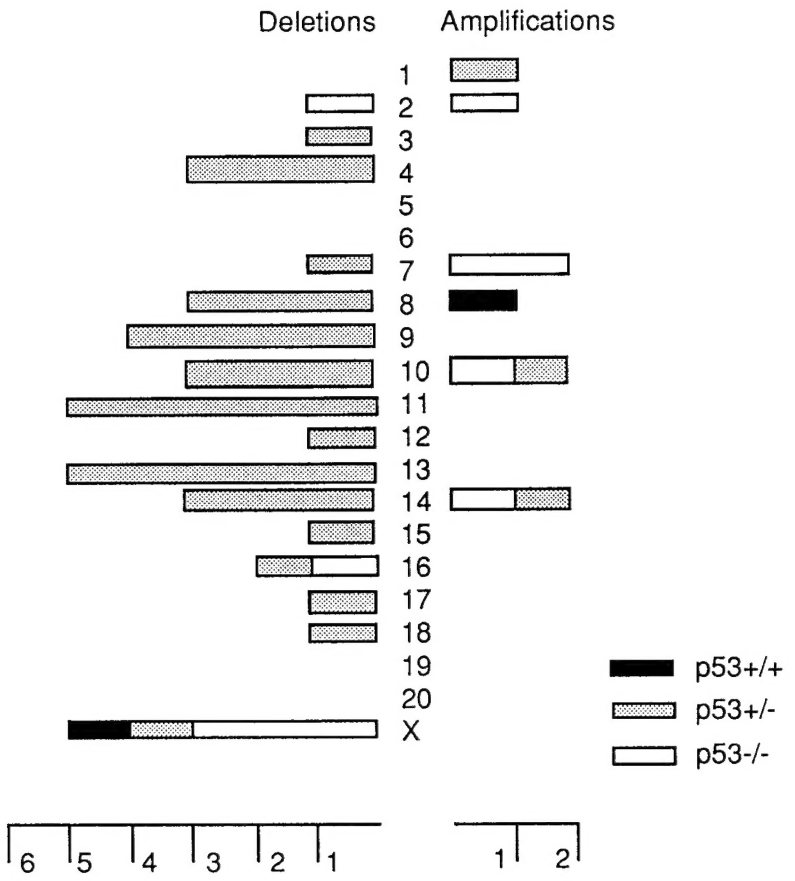

Figure 3. Chromosomal pattern of CGH DNA copy number gains and losses in the *Wnt-1 TG* p53 mammary tumors. CGH data from 25 *Wnt-1 TG* p53 tumors are compiled in this figure according to chromosome (listed in the middle column). The scale at the bottom indicates the number of tumors observed with a copy number gain or loss at a given chromosome. The p53 genotype of a tumor is indicated by black filling (p53+/+), shaded filling (p53+/-), or no filling (p53-/-).

The chromosomal abnormalities that were observed were both DNA copy number losses and gains, with losses predominating. Many of the copy number losses encompassed entire chromosomes or most of a chromosome. The pattern of chromosomal DNA gains and losses was at least partially non-random, with particular chromosomes displaying more frequent copy number gains and losses than others. These losses and gains are shown in Fig. 3. Note that DNA copy number losses were observed in at least four different tumors for chromosomes 9, 11, 13, and X. DNA copy number gains were observed at least twice on chromosomes 7, 10, and 14. Interestingly, in a *Wnt-1 TG* p53-/- tumor with evidence of DNA copy number gains on chromosome 7, we were able to demonstrate by Southern blot hybridization amplification (6-8 copies) of the *int-2/FGF3* gene (data not shown). This gene also was shown to be greatly increased in mRNA expression in this tumor. Since *int-2/FGF-3* has previously been activated in some mouse mammary carcinomas (Peters et al., 1986), this result not only validates the power of the CGH technique, it confirms the probable cooperation of *int-2/FGF-3* and *Wnt-1* in the generation of this tumor.

Chromosome 11 losses were usually associated with LOH of the wild type p53 allele in *Wnt-1 TG* p53+/- tumors, consistent with the location of the p53 gene on mouse chromosome 11. Fig. 3 also suggests that certain chromosomal losses tended to be associated with a particular p53 genotype. For example, the *Wnt-1 TG* p53+/- tumors showed losses in chromosomes 9 and 13, which were not observed in the *Wnt-1 TG* p53+/+ and *Wnt-1 TG* p53-/- tumors. In addition, half of the *Wnt-1 TG* p53-/- chromosomal abnormalities were increases in DNA copy number, whereas less than 10% of the chromosome alterations in the p53+/- tumors were increases in DNA copy number (Fig. 3). The CGH results confirm the cytogenetic data and support the hypothesis that loss of p53 results in increased genomic instability at the chromosomal and subchromosomal level.

DISCUSSION

This study represents our attempts to determine the effects of the presence or absence of p53 on tumor progression in a single targeted tissue. The results indicate that loss of p53 does have dramatic effects on both biological and genetic aspects of mammary tumor progression in our model. *Wnt-1* transgenic mice missing p53 (p53-/-) display (1) accelerated tumor development compared to *Wnt-1 TG* p53+/+ and *Wnt-1 TG* p53+/- mice; (2) altered tumor histopathology compared to p53+/+ mice; and (3) increased genomic instability compared to *Wnt-1 TG* p53+/+ mice. The *Wnt-1 TG* p53+/- mice, while not developing tumors any sooner than Wnt-1 p53+/+ mice, do exhibit altered mammary tumor histopathology (more anaplastic, less fibrotic) similar to the tumors of the *Wnt-1 TG* p53-/- mice when the remaining p53 wild type allele is lost. Surprisingly, the *Wnt-1 TG* p53+/- tumors with loss of the wild type allele display even more genomic instability (as measured by CGH) than *Wnt-1 TG* p53-/- tumors.

These *in vivo* tumorigenesis experiments extend previous *in vitro* studies which indicated that loss of p53 confers genomic instability. However, the existence of *Wnt-1 TG* p53-/- tumors with diploid karyotypes suggests that p53 loss predisposes a tumor cell to genomic instability rather than induces it directly. Evidence exists that p53 is a cell cycle checkpoint protein both at G1 and mitosis (Kastan et al., 1992; Livingstone et al., 1992; Yin et al., 1992; Cross et al., 1995). Cells which lose the p53-mediated mitotic spindle checkpoints may be likely to leave mitosis and enter G1 before completing chromosome segregation. Cross et al. (1995) have shown that the loss of the p53 mitotic checkpoint often results in tetraploid and octaploid cells *in vitro* and *in vivo*. Such results are consistent with our observations of hypotetraploidy in many of the *Wnt-1 TG* p53 mammary tumors.

Despite the correlation between loss of p53 and increased genomic instability in our model, it appears that increased genomic instability *per se* is not necessarily correlated with accelerated tumorigenesis. The tumors with the most chromosomal abnormalities, the *Wnt-1 TG* p53+/- (LOH) tumors, do not develop any sooner than *Wnt-1 TG* p53+/+ tumors, which show the least chromosomal instability. We hypothesize that chromosomal gains and losses which do occur may be selected for during tumor progression, but do not represent the key rate limiting events which determine the initial tumor formation.

One mechanism by which loss of p53 may confer accelerated tumorigenesis is through loss of p53-mediated apoptosis. Loss of p53 in other murine tumor models has been shown to result in decreased apoptosis of tumor cells and this has been correlated with increased rate and aggressiveness of tumor growth (Lowe et al., 1994; Symonds et al., 1994). Loss of p53-mediated apoptosis could explain the earlier appearance of the *Wnt-1 TG* p53-/- mammary tumors. However, why didn't the p53+/- (LOH) tumors show even slightly increased rates of tumor development over *Wnt-1 TG* p53+/+ tumors? One explanation is that loss of the remaining wild type allele is a relatively late event in tumor development, so that p53-mediated apoptosis is not lost in this type of tumor until it is too late to affect the time to overt tumor appearance. A second possibility is that p53 wild type allele loss does occur relatively early but that loss of p53-mediated apoptosis is not a rate limiting step to tumor formation in this particular model and that other mechanisms are crucial. Further experiments are currently underway to test both possibilities.

REFERENCES

Aldaz CM, Chen A, Gollahon LS, Russo J, Zappler K (1992): Nonrandom abnormalities involving chromosome 1 and Harvey-ras-1 alleles in rat mammary tumor progression. Cancer Res 52:4791-4798.

Clarke AR, Purdie CA, Harrison DJ, Morris RG, Bird CC, Hooper ML, Wyllie AH (1993): Thymocyte apoptosis induced by p53-dependent and independent pathways. Nature 352:849-852.

Cross SM, Sanchez CA, Morgan CA, Schimke MK, Ramel S, Idzerda RL, Raskind WH, Reid BJ (1995): A p53-dependent mouse spindle checkpoint. Science 267: 1353-1356.

Donehower LA, Harvey M, Slagle BL, McArthur MJ, Montgomery CA, Butel JS, Bradley A (1992): Mice deficient for p53 are developmentally normal but susceptible to spontaneous tumours. Nature 356: 215-221.

Finlay CA, Hinds PW, Levine AJ (1989): The p53 proto-oncogene can act as a suppressor of transformation. Cell 57: 1083-1093.

Greenblatt MS, Bennett WP, Hollstein M, Harris CC (1994): Mutations in the p53 tumor suppressor gene: clues to cancer etiology and molecular pathogenesis. Cancer Res 54: 4855-4878.

Harvey M, McArthur MJ, Montgomery CA, Butel JS, Bradley A, Donehower LA (1993): Spontaneous and carcinogen-induced tumorigenesis in p53-deficient mice. Nature Genet 5: 225-229.

Kallioniemi A, Kallioniemi O-P, Sudar D, Rutovitz D, Gray JW, Waldman F, Pinkel D (1992): Comparative genomic hybridization for molecular cytogenetic analysis of solid tumors. Science 258: 818-821.

Kastan MB, Zhan Q, El-Deiry WS, Carrier F, Jacks T, Walsh WV, Plunkett BS, Vogelstein B, Fornace AJ Jr (1992): A mammalian cell cycle checkpoint pathway utilizing p53 and GADD45 is defective in ataxia-telangiectiasia. Cell 71: 587-597.

Livingstone LR, White A, Sprouse J, Livanos E, Jacks T, Tlsty T (1992): Altered cell cycle arrest and gene amplification potential accompany loss of wild-type p53. Cell 70: 923-935.

Lowe SW, Schmitt EM, Smith SW, Osborne BA, Jacks T (1993a): p53 is required for radiation-induced apoptosis in mouse thymocytes. Nature 362: 847-849.

Lowe SW, Ruley HE, Jacks T, Housman DE (1993b): p53-dependent apoptosis modulates the cytotoxicity of anticancer agents. Cell 74: 957-967.

Lowe SW, Bodis S, McClatchey A, Remington L, Ruley HE, Fisher DE, Housman DE, Jacks T (1994): p53 status and the efficacy of cancer therapy *in vivo*. Science 266: 807-810.

Malkin D, Li FP, Strong LC, Fraumeni JF Jr, Nelson CE, Kim DH, Kassel J, Gryka MA, Bischoff FZ, Tainsky MA, Friend SH (1990): Germ line p53 mutations in a familial syndrome of breast cancer, sarcomas, and other neoplasms. Science 250: 1233-1238.

Srivastava S, Zou Z, Pirollo K, Blattner W, Chang EH (1990): Germ-line transmission of a mutated p53 gene in a cancer prone family with Li-Fraumeni syndrome. Nature 348: 747-749.

Symonds H, Krall L, Remington L, Saenz-Robles M, Lowe S, Jacks T, Van Dyke T (1994): p53-dependent apoptosis suppresses tumor growth and progression *in vivo*. Cell 78: 703-711.

Tsukamoto AS, Grosschedl R, Guman RC, Parslow T, and Varmus HE (1988): Expression of the *int*-1 gene in transgenic mice is associated with mammary gland hyperplasia and adenocarcinomas in male and female mice. Cell 55: 619-625.

Yin H, Tainsky MA, Bischoff FZ, Strong LC, Wahl GM (1992): Wild-type p53 restores cell cycle control and inhibits gene amplification in cells with mutant p53 alleles. Cell 70: 937-948.

Yonish-Rouach E, Resnitzky D, Lotem J, Sachs L, Kimchi A, Oren M. (1991): Wild-type p53 induces apoptosis of myeloid leukemic cells that is inhibited by interleukin-6. Nature 352: 345-347.